



Working Report 2010-61

# GPS Measurements in Satakunta Area

Markku Poutanen

Sonja Nyberg

Joel Ahola

October 2010

**Working Report 2010-61**

# **GPS Measurements in Satakunta Area**

**Markku Poutanen**

**Sonja Nyberg**

**Joel Ahola**

**Finnish Geodetic Institute**

**October 2010**

Base maps: ©National Land Survey, permission 41/MML/10

---

Working Reports contain information on work in progress  
or pending completion.

The conclusions and viewpoints presented in the report  
are those of author(s) and do not necessarily  
coincide with those of Posiva.

## **GPS Measurements in Satakunta Area**

### **ABSTRACT**

The Finnish Geodetic Institute, the Geological Survey of Finland, Posiva Ltd and municipalities in the district of Satakunta launched the GeoSatakunta research program in 2002 to carry out interdisciplinary studies on regional bedrock stress field and to apply the results e.g. in land use planning in the Satakunta area. The area was chosen for many reasons. Its geological diversity, extensive multi-disciplinary data coverage, and various interests of participants made the area suitable for the project. The purpose of the GPS observations is to get detailed information on recent crustal deformations in the area. The Finnish Geodetic Institute maintains e.g. national GPS network, FinnRef, and since 1995 a local research network in the Olkiluoto area. The Satakunta network differs from these, and this is the first time to obtain such detailed information of a regional network in Finland.

The Satakunta GPS network consists of 13 concrete pillars for episodic GPS campaigns and the Olkiluoto permanent GPS station in the FinnRef network. The distances between the concrete pillars are 10-15 km, and the sites were chosen in a co-operation with the Geological Survey of Finland taking into account the geological structures in the area. The City of Pori made the final reconnaissance in the field and constructed eight pillars in 2003. The original network was expanded in 2005-2006 in Eurajoki and Rauma, and at the City of Rauma joined the co-operation. The five new pillars join the previous Olkiluoto network into the Satakunta network. There have been three annual GPS campaigns in 2003-2008.

Time series of the Satakunta network are shorter than in the Olkiluoto network, and also the distances are longer. Therefore, the same accuracy than in Olkiluoto has not yet achieved. However, mm-sized movements can be excluded. Estimated velocities were small (0.2 mm/a) and mostly statistically insignificant because of relatively short time series.

In this publication we describe the background of the GPS measurements, introduce the GeoSatakunta GPS network, discuss the GPS processing and present the results of the time series analysis. More measurement campaigns are anticipated in the future but it is not necessary to carry out measurements as frequently. Observing every 2-3 years one can monitor long-term trends but the epoch of abrupt movements are not possible to get accurately.

The GPS network can be used also as a reference for the cities and municipalities in the area. It is the most accurately measured regional network in Finland and its free access and open structure allows the use for many common purposes.

**Keywords:** Bedrock movement, GPS measurements, Satakunta area

## GPS-mittaukset Satakunnan alueella

### TIIVISTELMÄ

Geodeettinen laitos aloitti GeoSatakunta-projektiin liittyvät GPS-mittaukset Pori-Olkiluoto -alueella vuonna 2003 ja mittausten yhtenä tavoitteena on ollut saada tietoa Satakunnan kallioperän nykyhetken liikunnoista. Monitieteiseen projektiin ovat osallistuneet Geologian tutkimuskeskus, Geodeettinen laitos, Posiva Oy, sekä Porin ja Rauman kaupungit. EU-rahoitusta on saatu Satakuntaliiton kautta. Geologisesti Satakunnan alue on hyvin mielenkiintoinen ja siitä on olemassa huomattava määrä eri menetelmin kerättyä havaintoaineistoa. Kallioperän liikunnoista näin laajalla alueella ei tähänastisilla havainnoilla ole kuitenkaan voinut saada tietoa. Geodeettinen laitos ylläpitää maanlaajuista GPS-verkkoa ja on tehnyt GPS-mittauksia Olkiluodon alueella Posiva Oy:n tilaustutkimuksena muutaman kilometrin laajuisessa paikallisverkossa vuodesta 1995 lähtien. Satakunnan verkon mittausten luonne poikkeaa sekä valtakunnan laajuisesta että Olkiluodon paikallisesta tutkimusverkosta, eikä vastaavaa alueellista tutkimusta ole Suomessa aiemmin tehty.

Tarkkoihin GPS-mittauksiin suunniteltu verkko käsittää kaikkiaan 14 pysyvää betonipilaria, joista yksi on valtakunnallisen FinnRef-verkon pysyvä asema ja alkuperäinen Olkiluodon verkon piste. Keskimäärin 10-15 km välein olevien pilarien paikat valittiin yhteistyössä Geologian tutkimuskeskuksen kanssa ottaen huomioon mm. alueen geologinen rakenne. Porin kaupunki teki pisteiden rakennuspaikkojen valinnan maastossa sekä rakensi havaintopilarit. Alkuperäistä kahdeksan pisteen verkkoa laajennettiin vuosina 2005-2006 Eurajoelle ja Raumalle viidellä uudella pilarilla. Samalla yhteistyöhön saatiin mukaan Rauman kaupunki. Uudet pilarit yhdistävät myös Olkiluodon paikallisverkon Satakunnan verkkoon.

Satakunnan verkon aikasarjat ovat Olkiluotoa lyhyemmät ja pilarien välimatkat pitempiä, joten samaan tarkkuuteen ei mittauksissa ole vielä päästy. Kuitenkaan millimetrituokkaa olevia liikkeitä ei ole havaittu. Suurimmat laskennallisesti saatavat liikkeet ovat luokkaa 0.2 mm/v, mutta tähänastisista aikasarjoista ei voi tilastollisesti luotettavasti määrittää näin pieniä liikkeitä.

Tässä julkaisussa kuvataan Satakunnan alueen GPS-verkon rakentamiseen liittyvät taustat, verkon rakentaminen, GPS-mittaukset ja mittausten tulokset ja analyysi. Mittauksia on tarkoitus jatkaa myös tulevaisuudessa. Vuoteen 2008 saakka havaintoja on tehty kolme kertaa vuodessa, mutta tulevaisuudessa 2-3 vuoden välein. Monitoroinnilla voidaan selvittää pitkäaikaiset liikunnat nykyistä tarkemmin, mutta ei esimerkiksi äkillisten liikkeiden tarkkaa ajankohtaa.

GPS-verkkoa käytetään myös alueen kuntien ja kaupunkien kiintopisteverkkona. Se on tarkimmin mitattu ja tunnettu alueellinen GPS-verkko Suomessa. Verkon pilarien avoin rakenne mahdollistaa hyödyntämisen myös tällaiseen tarkoitukseen.

**Avainsanat:** Kallioliikunnot, GPS-mittaukset, Satakunta

## TABLE OF CONTENTS

ABSTRACT

TIIVISTELMÄ

1. BACKGROUND .....	3
2. SOME EARLIER AND RELATED GEODETIC STUDIES.....	7
2.1 The Baltic Sea Level Campaign .....	7
2.2 BIFROST project.....	8
2.3 Finnish permanent GPS network FinnRef <sup>®</sup> and the Nordic Geodetic Observing System NGOS.....	9
2.4 Deformation studies at Olkiluoto.....	10
2.5 DynaQlim and RCD-LITO.....	14
3. GPS OBSERVING ERRORS.....	17
4. GEOSATAKUNTA GPS NETWORK AND MEASUREMENTS.....	23
4.1 Network planning and site selection .....	23
4.2 GPS pillars .....	23
4.3 Control markers.....	32
4.4 Equipments and measurement campaigns.....	33
5. COMPUTATION .....	37
5.1 Computation software and strategy.....	37
5.2. GPS processing results.....	38
6. DATA ANALYSIS.....	41
6.1. Vector time series .....	41
6.2. Deformation analysis.....	44
7. CONCLUSIONS AND THE FUTURE.....	49
ACKNOWLEDGEMENTS .....	51
REFERENCES .....	53
APPENDIX 1 .....	57
APPENDIX 2 .....	61



## 1 BACKGROUND

The Finnish Geodetic Institute (FGI), the Geological Survey of Finland (GSF), Posiva Ltd and municipalities in the district of Satakunta started the GeoSatakunta research program in 2002. A preceding project was initiated already in the year 2000. The purpose of the GeoSatakunta project is to get detailed information on recent crustal deformations in the area, study the geological structures and get information on the stress fields (Ahola & Poutanen 2006). In 2008-2009 the project was called InnoGeo.

The Satakunta area was chosen for many reasons. Its geological diversity, extensive multi-disciplinary data coverage, and various interests of participants made the area suitable for the project. In the geological side, the connections of Jotnian sandstone, Postjotnian diabase and the world famous Rapakivi granite are of main interest. An old shear zone of Kynsikangas begins from the Mid-Atlantic ridge, and it has been under a large deformation during the Svekofennian Orogen.

Plate tectonic reconstructions indicate that the area belongs to the early Proterozoic Southern Finland and Central Finland continental arcs. Collision of these arc complexes took place 1890 - 1880 Ma ago. The sandstone is bounded on both sides by fault zones and the age of the sandstones is at least 1400-1300 Ma. The zone is cut by younger Postjotnian olivine diabase dykes, 1270-1250 Ma in age. The age of the intruded Rapakivi granites is estimated to be 1580-1550 Ma (Paulamäki et al. 2002). In Figure 1-1 there is the geological structure of the area and a schematic diagram of the crustal structure.

The Proterozoic bedrock in the Gulf of Bothnia is to a great extent covered by younger sediments (Hutri 2007). The area contains several deep fracture zones that divide the bedrock into various separate blocks. Palaeoseismic faults in the sediments, dated to the early Holocene, about 10500 B.P., indicate that when the Late Weichselian ice sheet was retreating, bedrock stresses were released along the ancient fracture zones (Hutri 2007). Contemporary, the major element that deforms the crust in Fennoscandia is the Glacial Isostatic Adjustment (GIA). Since the last glaciation there has been the crustal rebound. Currently, it is about 7 mm/a in this area. From NW to SE of the area, the uplift rate changes about 1 mm/a. Such a gradient should have some effect over time on the stress field of the crust.

There are also other processes that are either slower or smaller in magnitude than the glacial-related processes. These can play an important role in long time scales or they can cause abrupt motions (earthquakes) when monitored over very long time spans. As listed in (Lambeck & Purcell 2003) these include erosion and sedimentation redistributed surface loads and stress on the crust, plate tectonic forces, including the Mid-Atlantic push, that can contribute to the regional stress, geological anomalies of the crust and lithosphere causing them to be in a non-equilibrium state and therefore introducing stress fields. Climate-change processes will cause actual changes in the sea level and water mass in addition to the relative sea-level change due to the postglacial rebound. All these signals are mixed together, causing both geometrical changes (vertical and horizontal displacements, local deformations, sea level change) and changes in gravity.

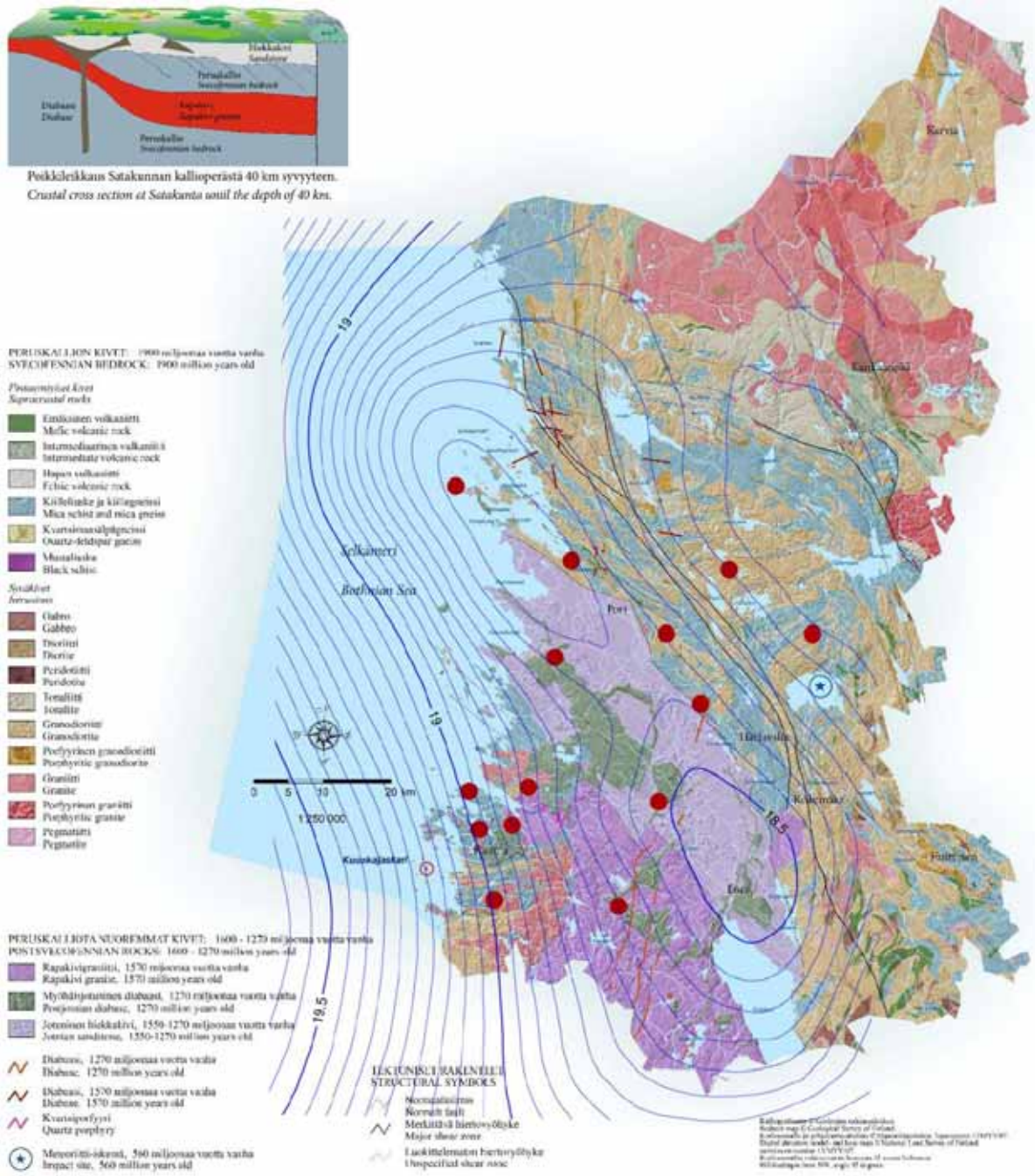


**Figure 1-1.** Geological structure of the Satakunta area. On top of the map there are the approximate positions of the GeoSatakunta GPS network points, and the contour lines of the geoid. Base map © Geological Survey of Finland ([www.pori.fi/geosatakunta](http://www.pori.fi/geosatakunta)), FIN2005 geoid model by Mirjam Bilker-Koivula (2009).

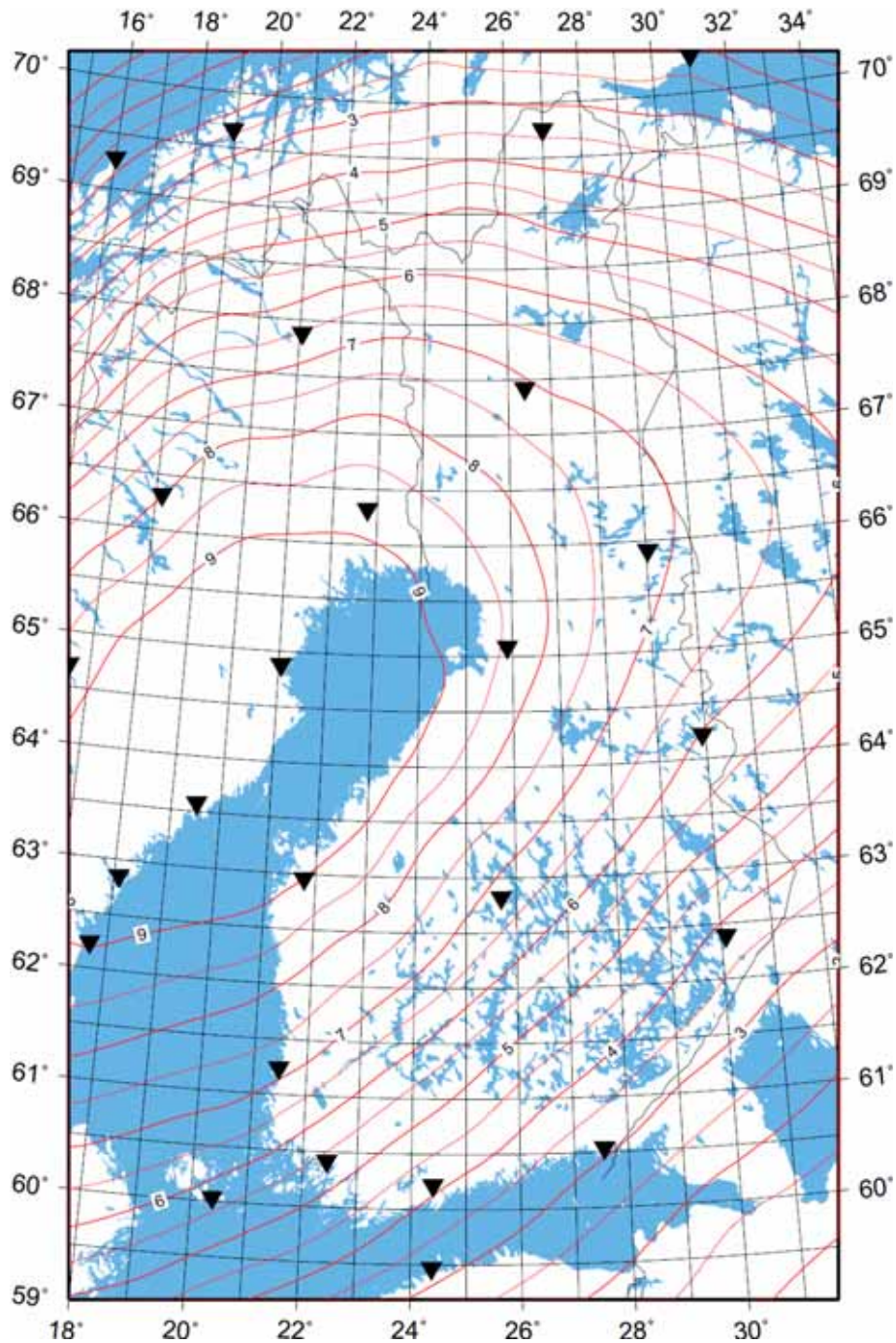


**Figure 1-2.** Contemporary postglacial rebound in Finland in [mm/a], relative to the centre of the Earth. We have applied the Nordic NKG2005LU model (Vestøl 2006, Ågren and Svensson, 2007) relative to the mean sea level at the Baltic tide gauges in 1892–1991. This was converted to the absolute vertical velocities by  $h_{abs} = 1.06(h_{rel} + 1.3 \text{ mm/y})$ . The formula takes into account the mean eustatic rise of the Baltic Sea during the last century and the rise of the geoid. Triangles show the permanent GNSS stations.

Lambeck and Purcell (2003) published an overview of the glacial stress and crustal rebound in Finland. They conclude that with current models realistic regional stress patterns can be predicted, and any crustal failure triggered by glacial loading and unloading will have occurred preferentially when a region became ice-free. They also conclude that the potential for reactivating faults today is negligible. As shown by the work of Hutri (2007), there has been faulting during the Holocene near the ancient fracture zones, possibly in connection of the ice retreat.

Contemporary deformation status of the Satakunta bedrock is unknown. The land uplift in the Satakunta area is between 6.5 – 7.5 mm/a (Figure 1-2). The 1 mm/a gradient in the area, combined with other deforming forces and complex crustal structure give rise to stress field which may cause deformation in the upper crust. Currently, no extensive seismic activity exists in the area (Seismo 2007). Expected deformation is presumably small, slow, or occur only occasionally. Therefore, long-lasting geodetic monitoring over a larger area is needed to recover the possible phenomena.

Geodesy is the key provider of data and accurate measurements needed for global, regional and local research of contemporary deformation, sea level and gravity change. Reliability of the results is based on a stable, well-defined global geodetic reference frame in which the precise observations are made. Space geodetic technique, especially GPS (or more generally, GNSS, *Global Navigation Satellite Systems*), has proved to be invaluable in this. The geodetic observations, especially repeated GPS observations described in this publication, will contribute to the detailed information about recent crustal movements in the area (Ahola & Poutanen 2006, Poutanen 2005).

With the GNSS techniques, positions and change rates of network stations can be accurately determined from regular measurement campaigns or continuous observations. This suggests that the components of deformation measures (such as the stress or strain tensor) can be estimated from the highly accurate geodetic data and analysed by means of the proper statistical testing procedures. The eigenspace components of these random deformation tensors (principal components, principal directions) are of focal interest in geodesy, geology, and geophysics. They play an important role in interpreting the geodetic-geodynamic-geophysical phenomena like earthquakes (seismic deformations), plate motions and crustal deformations among others.

National gravity networks have been maintained with relative gravimetric measurements. There have been only a limited number of absolute gravity points. In recent years, possibilities to make absolute measurements have been improved. We are moving toward the situation where the primary reference network is maintained by absolute measurements and the sites are common with those of other techniques, e.g. permanent GNSS stations. Measuring the secular change of gravity in a gravimetric network of permanent stations over long periods of time affords a unique method to monitor large-scale mass movements. In order to resolve models of mass redistribution in glacial isostatic rebound models, gravity change needs to be determined at 1 to 2 nm/s<sup>2</sup>/a reproducibility.

In the following we will describe some previous geodetic measurements related to the Satakunta area, discuss methods in GPS determination and describe the establishment of the GPS network in the area and give the results of the observations.

## 2 SOME EARLIER AND RELATED GEODETIC STUDIES

### 2.1 The Baltic Sea Level Campaign

The first GPS-based study in the area was the *Baltic Sea Level* (BSL) project. It was initiated in the Scientific Assembly of the IAG (*International Association of Geodesy*) in Edinburgh in 1989 and it lasted until the IUGG (*International Union of Geodesy and Geophysics*) General Assembly in Birmingham in 1999. Goals of the Baltic Sea Level Project included unification of the vertical datums in the countries around the Baltic Sea, to contribute to the determination of the gravity field and the geoid in the Baltic Sea region, to determine the sea level and sea surface topography of the Baltic Sea, to monitor postglacial rebound, especially in the sea area, and to re-measure the Baltic Ring for horizontal crustal deformation studies.

Series of repeated GPS measurements were performed in 1990 (BSL I), 1993 (BSL II) and 1997 (BSL III). The network of BSL III is shown in Figure 2-1. The BSL III was arranged simultaneously with the EUVN (*European Vertical GPS Reference Network*) GPS campaign. The total number of stations was about 60. Details and results of the BSL GPS campaigns are published in Kakkuri 1994, 1995, Kakkuri & Poutanen 1997, Poutanen & Kakkuri 1999, and Poutanen 2000.

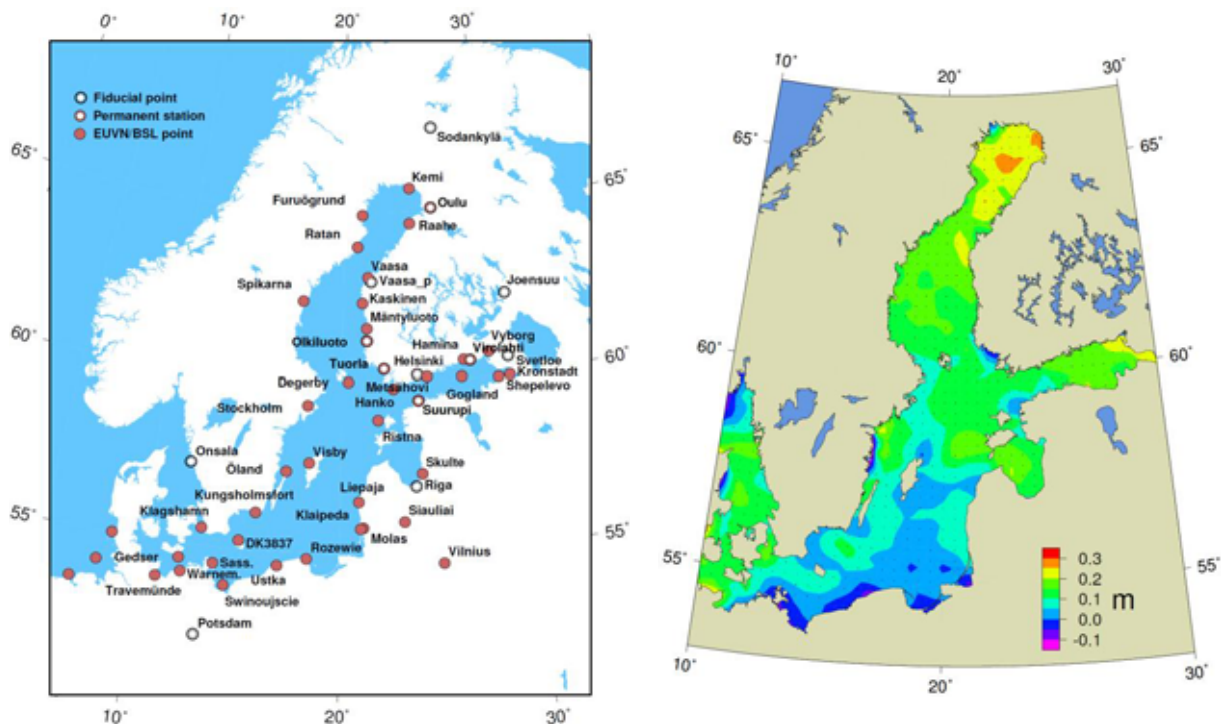


**Figure 2-1.** (Left): Network of the BSL97 GPS campaign. (Right): Sea Surface Topography as determined from the BSL GPS campaigns and ERS1 and ERS2 satellite altimetry data. (Poutanen 2000).

## 2.2 BIFROST project

*Baseline Inferences for Fennoscandian Rebound Observations, Sea Level, and Tectonics* (BIFROST) has been a project that was initiated already in 1993 taking advantage of tens of permanent GPS stations both in Finland and Sweden. Researchers in United States, Canada, Great Britain, Sweden and the Finland take part in the BIFROST project. The main BIFROST results are published in Milne et al. 2001 and 2004, Johansson et al. 2002, and Scherneck et al. 2002. Longer GPS time series were published by Lidberg (2007).

The goal of BIFROST is to measure the contemporary crustal deformation in Fennoscandia and provide a new GIA (Glacial Isostatic Adjustment) observable for determination of the Earth structure and Fennoscandian ice history. The project aims at inference of absolute sea level change by combination of the vertical rates with tide gauge derived relative sea level rates. The project also expects to reveal horizontal motion, and possible perturbation due to other sources of stress, generally covered under the term of neotectonics or intraplate tectonics (Figure 2-2).

As the result of the BIFROST studies (Johansson et al. 2002, Milne et al. 2001, 2004, Scherneck et al. 2002) of the Fennoscandian postglacial rebound mechanism, we know that in addition to the land uplift, there is also a horizontal component of motion, where the surface of the Earth's crust moves away from the uplift centre at a speed of about 10 % of the uplift rate. Due to the sparse network, BIFROST is unable to give detailed information in our area of interest.

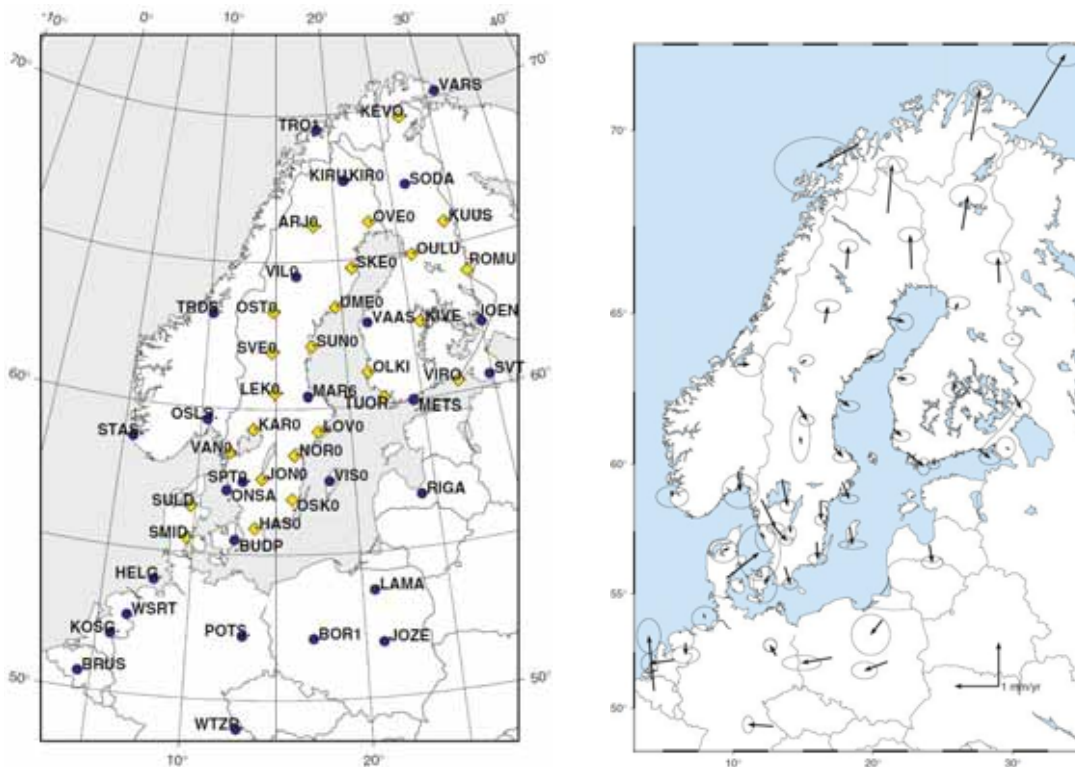


**Figure 2-2.** (Left): Network of the BIFROST project covers more than 50 permanent GPS stations. (Right): Horizontal velocity differences of the Milne GIA model minus GPS estimates. Lidberg (2007).

### 2.3 Finnish permanent GPS network FinnRef<sup>®</sup> and the Nordic Geodetic Observing System NGOS

The Finnish permanent GPS network FinnRef<sup>®</sup> consists of 13 permanent GPS stations. The distances between the stations are 100-200 km. The network is the backbone of the Finnish realisation of the European coordinate reference system ETRS89, referred as to EUREF-FIN. Most of the stations have been operational since 1996 offering now a possibility for 10-year long time series.

Four stations in the FinnRef<sup>®</sup> network (Metsähovi, Vaasa, Joensuu, Sodankylä) belong to the *EUREF permanent GNSS network (EPN)*, and one station (Metsähovi) belongs to the network of the *International GNSS Service (IGS)* of the IAG. Through these stations FinnRef creates a connection to the global reference frames and the stations are used for maintaining global reference frames as well as geodetic and geodynamic studies (Koivula 2006, Mäkinen et al. 2003, Ollikainen et al. 1997).

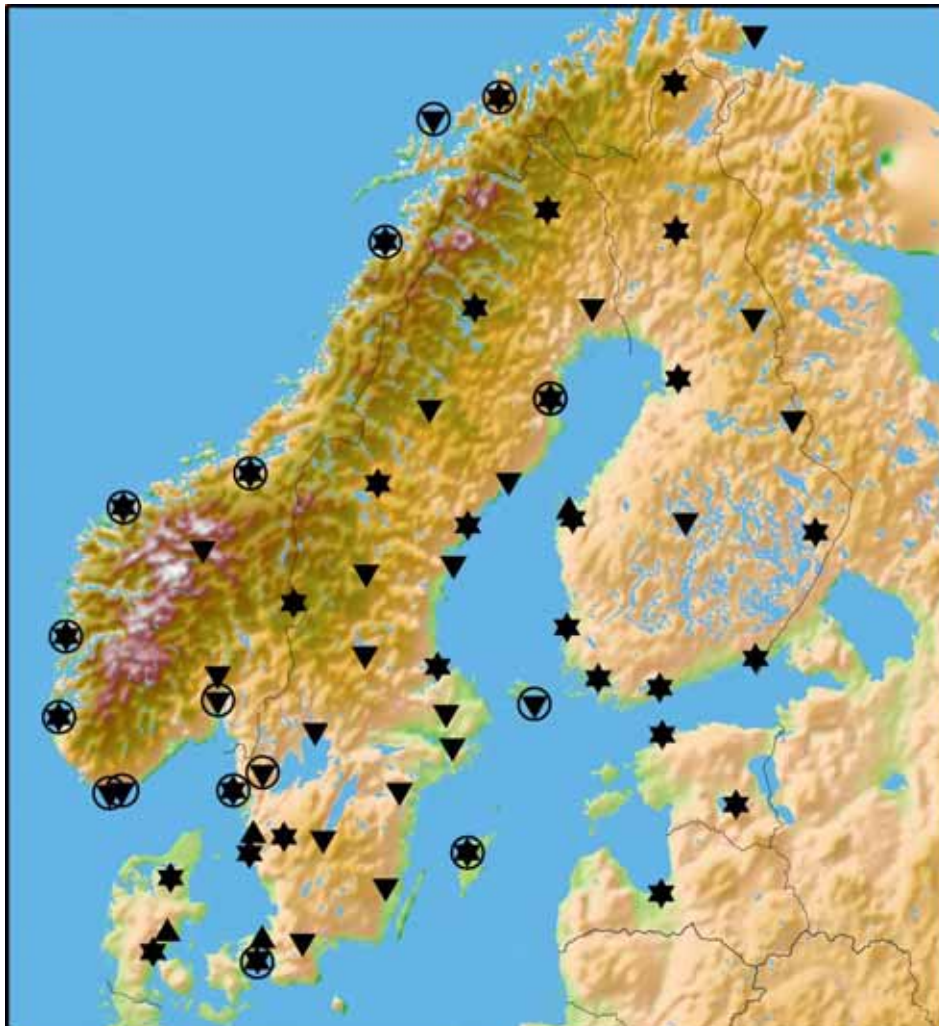


**Figure 2-3.** Network of the Nordic Geodetic Observing System NGOS. Upside-down triangles show permanent GNSS stations, triangles sites included in the NGOS absolute gravity plan, and circles denote tide gauges included in the NGOS. The Finnish permanent GNSS network FinnRef<sup>®</sup> consists of 13 stations shown on the map.

All FinnRef<sup>®</sup> stations are used in the computation of the joint Nordic GNSS network and they enable the study of the crustal motions of the Earth. The absolute gravity observations have been made at eight GPS stations, viz. in Metsähovi, Vaasa, Joensuu, Olkiluoto, Virolahti, Kevo, Kuusamo and Sodankylä with the FG5 gravimeter owned by the FGI.

GPS and gravity observations made on the permanent GPS stations are a part of the Nordic Geodetic Observing System, NGOS. Established by the Nordic Geodetic Commission, NGOS is planned to be a regional implementation and densification of the Global Geodetic Observing System, GGOS (Poutanen et al. 2005, 2007). NGOS will contribute to the GGOS and other IAG Services, provide the reference frames for the Nordic countries, as well as contribute to the global ones, support scientific projects related to the geodynamics of the Nordic area and provide ground-truth for satellite missions. NGOS aims to provide geodetic observations for the Nordic area that are of sufficient quantity and quality to serve most of the needs of global Earth observation as well as practical and scientific applications in the region. For the Nordic countries, a main focus will be on crustal motion, dynamics of glaciated areas and sea level.

Although FinnRef<sup>®</sup> or NGOS network is too sparse for studies in the Satakunta area (only Olkiluoto is inside the area), it forms the basic reference in the Nordic area for all geodynamics studies. Stability of the network is of ultimate importance to any GNSS-related work. Adding the gravity information, one has a possibility to get more detailed information on the processes in lithosphere and upper mantle. Olkiluoto is also a reference station on GPS observations in the area.

## 2.4 Deformation studies at Olkiluoto

GPS based deformation studies have been made at the investigation areas of Posiva since 1994, when the network of ten GPS pillars was established at Olkiluoto (Chen and Kakkuri, 1995). The network of seven GPS pillars was built at Kivetty and Romuvaara during the year 1996. One pillar in each investigation area belongs to the Finnish permanent GPS network, FinnRef<sup>®</sup>.

The GPS network at Olkiluoto was extended in 2003 and 2005. Including the new pillars the local GPS network at Olkiluoto consists of 14 stations (Figure 2-4). The new pillars were built close to Kuivalahti, Taipalmaa and Hankkila villages and on a small island of Iso Pyrekari. According to the geological evidence it is expected that a fracture zone is located between the new stations, thus enabling the determination of possible deformations along the fracture zone. The new pillars have been observed since 2003 and 2005, but the time series are still too short for reliable deformation studies.

The whole network at Olkiluoto is measured twice a year (Figure 2-5). A total of 24 GPS campaigns have been carried out since 1995 (Ahola et al. 2008). There are five pillars, which have statistically significant horizontal velocities at Olkiluoto. These local velocity components are small but taking into account the standard deviations the largest velocity components seems to be reliably determined (maximum velocity is 0.20 mm/a  $\pm$  0.03 mm/a), see Figure. 2-6.

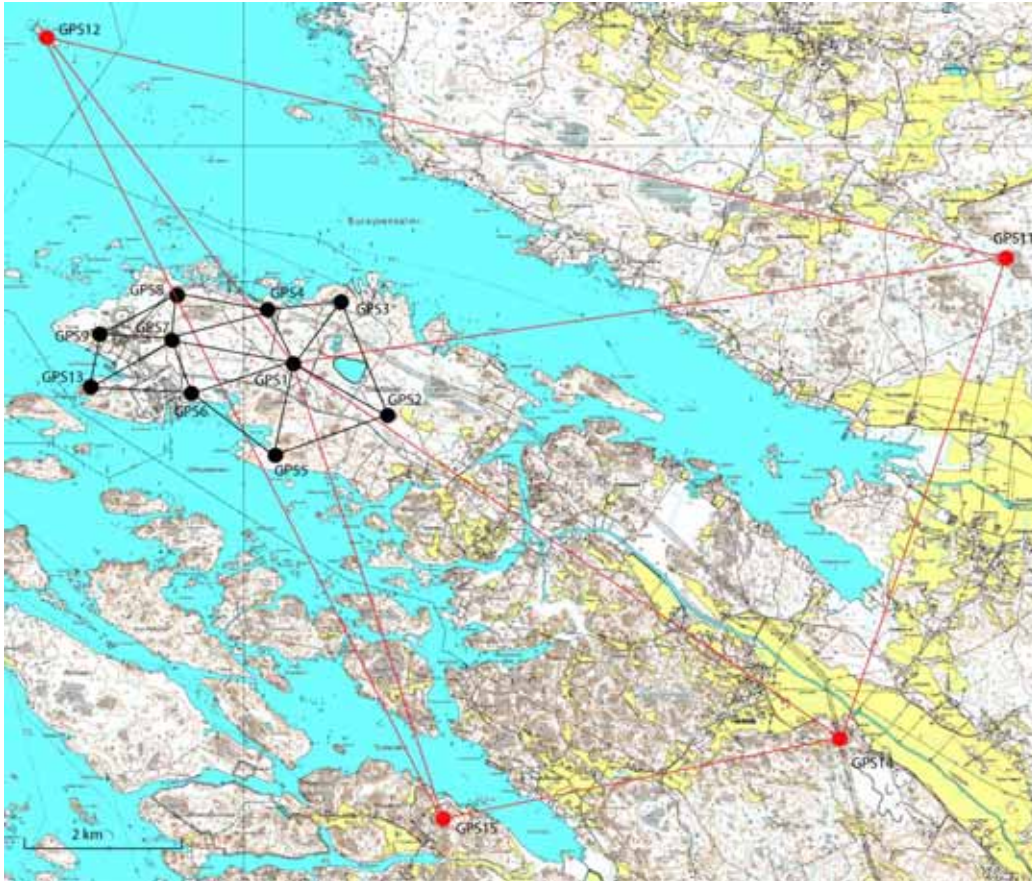


**Figure 2-4.** The local GPS monitoring network at the investigation area of Olkiluoto. Black: Original network has been established in 1994 (GPS13 in 2003). Red: Pillars have been established in 2003 and 2005.



**Figure 2-5.** GPS measurements at Olkiluoto. (Photograph T. Ahola)

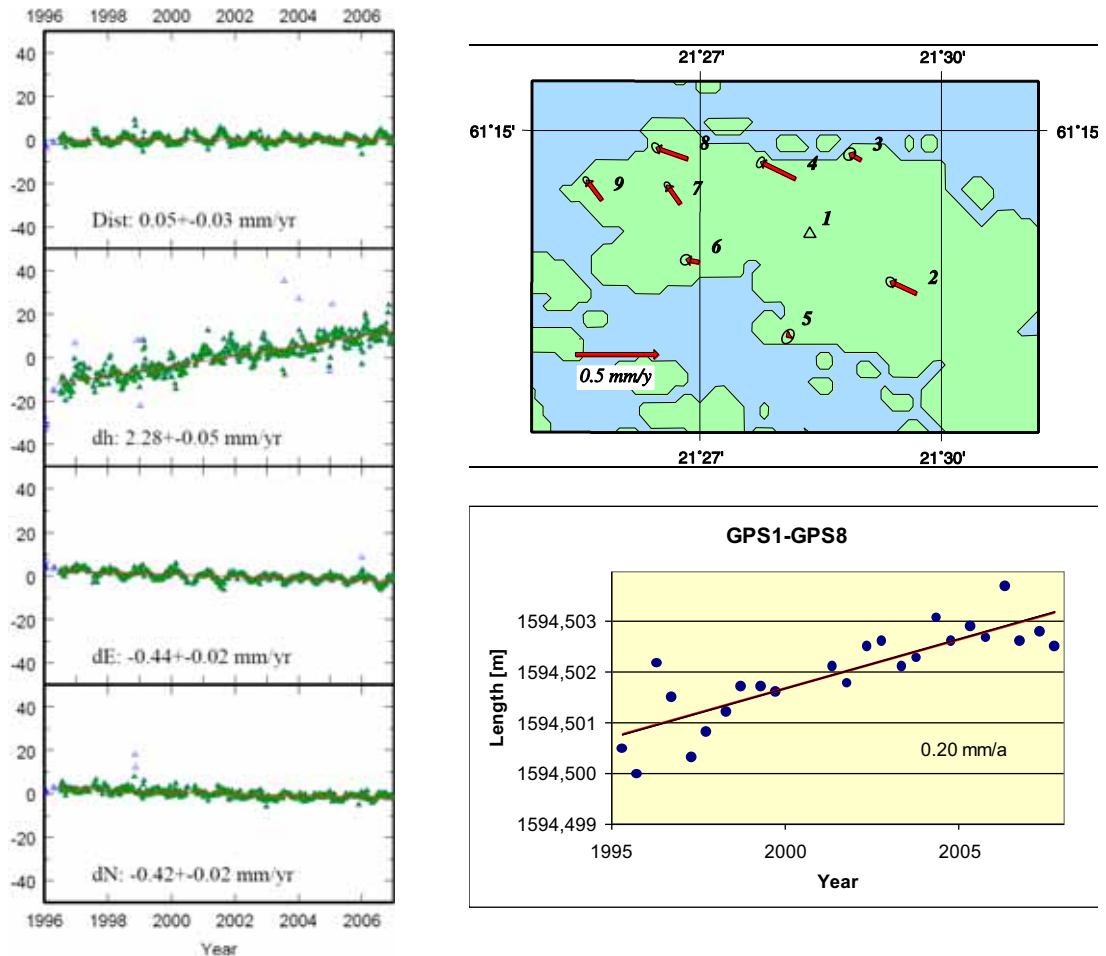


**Figure 2-6.** (Left): Time series of Metsähovi-Olkiluoto vector components. From top to bottom: baseline length, height, East, and North components. (Right) The most significant change rate ( $0.20$  mm/a  $\pm$   $0.03$  mm/a) at Olkiluoto is between the pillars GPS1 and GPS8 (Ahola et al. 2007 and 2008).

The uniform scale for the GPS measurements made in different years is the basic condition for reliable results in the deformation analyses. At Olkiluoto a baseline for electronic distance measurements (EDM) was built in 2002. The baseline has been measured using EDM instruments simultaneously with the GPS observations. The comparison between the GPS and EDM results can solve a possible scale error of the GPS.

GPS measurements are suitable to determine horizontal deformations, but the accuracy of height determination is not adequate. The FGI started to determine possible vertical deformations at Olkiluoto with precise levelling in 2003 (Figure 2-7). Levelling campaigns will be performed every second year and they are reported in separate working reports (Lehmuskoski 2004, 2006, 2008). Levelling shows of about  $0.6$  mm/a anomalous uplift rate between the precise levelling benchmark 51301 in Lapijoki and the 03219 on the Olkiluoto Island, about  $13$  km from each other (Figure 2-8). There is an additional  $0.15$  mm/a rate between 51301 and 03219 due to the land uplift difference, not shown on this plot. Moreover, the Northern part of the Olkiluoto Island is lifting  $0.2 - 0.3$  mm/a relative to the Southern part, see Figure 2-8. (Lehmuskoski 2008)



*Figure 2-7. Precise levelling at Olkiluoto. (Photograph J. Ahola.)*

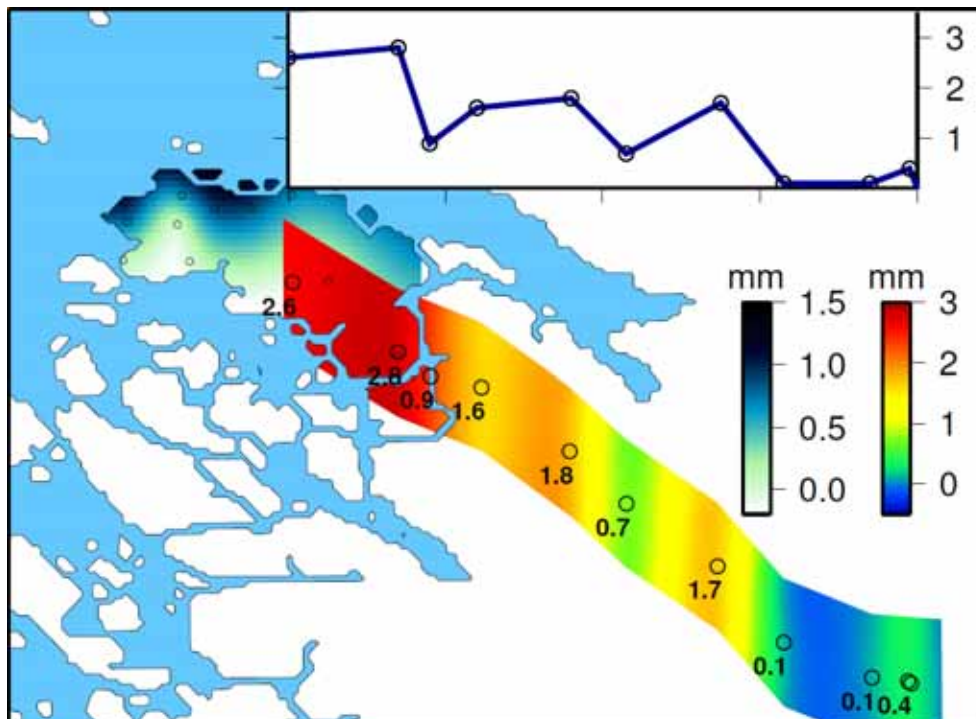


*Figure 2-8. Anomalous height change (in mm) at Olkiluoto based on repeated precise levelling during the four year period 2003-2007 (Lehmuskoski, 2008). The inserted profile shows that the change has happened mainly on two places. The colour shade on the Olkiluoto Island shows the tilt of the island during the same time, based on the repeated levelling between the GPS pillars.*

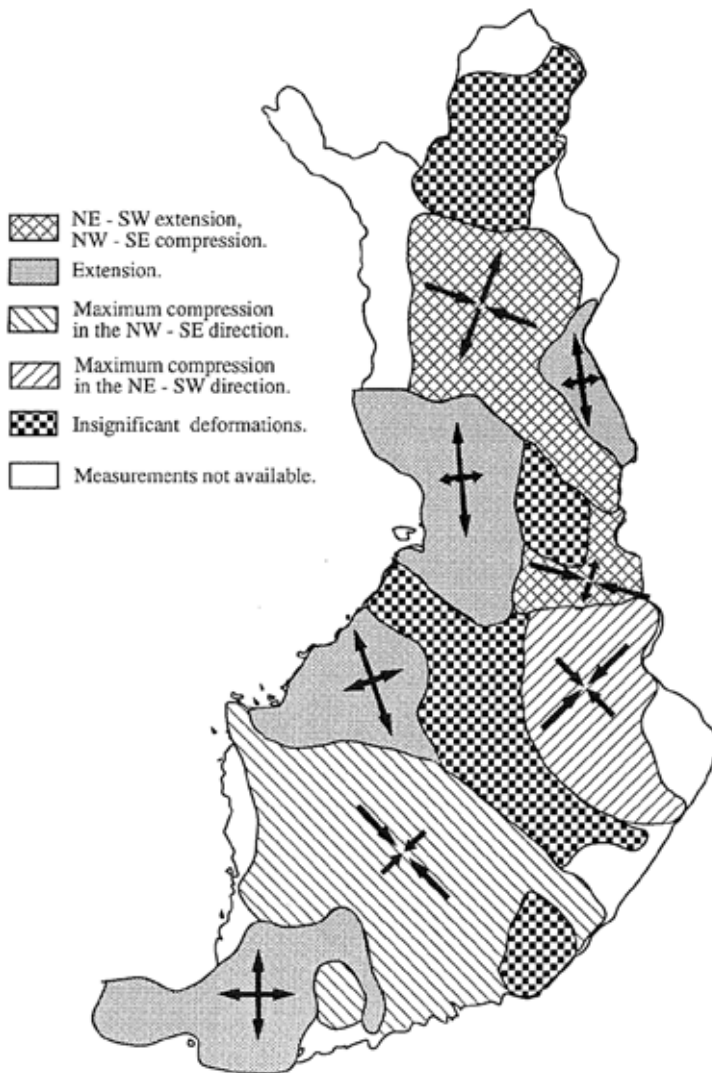


*Figure 2-9. A simplified pattern on stress and strain in Finland based on deformation studies by Chen (1991).*

## 2.5 DynaQlim and RCD-LITO

Chen (1991) published a study on crustal deformation in Finland using the triangulation data. The accuracy of triangulation is not sufficient for any detailed study in spite of the long time span. However, Chen showed regions with compression or extension; some of these coinciding with known crustal structures (Figure 2-9). This pattern is still to be confirmed.

With modern space geodetic techniques, accuracies will be at least one or two order of magnitudes better thus enabling a much shorter time series. Currently, there is an ongoing project RCD-LITO, funded by the Academy of Finland, where one hundred points observed with GPS in ten years interval will be used for a similar study. As a cooperation with the University of Stuttgart, we have used data from the Finnish Permanent GPS network FinnRef to compute the deformation tensors in Finland (Cai et al. 2007). In addition to the country-wide network, the other part of the RCD-LITO project concentrates to the Satakunta region in the *GeoSatakunta* project.

The RCD-LITO is under the umbrella of a global project: *Upper Mantle Dynamics and Quaternary Climate in Cratonic Areas, DynaQlim*. Aim of the DynaQlim is to understand the relations between the upper mantle dynamics, mantle composition, physical properties, temperature and rheology, to study the postglacial uplift and ice thickness models, Quaternary climate variations and Weichselian (Laurentian and other) glaciations during the late Quaternary (DynaQlim, 2008). Improved knowledge of the Earth's mantle and its coupling to the lithosphere and to the surface is a key to understand forces that generate these features.

The idea for the DynaQlim was first developed in the Finnish National Lithosphere Committee (Poutanen et al. 2006) and it was accepted as an ILP (International Lithosphere Program) regional co-ordination committee in 2007. DynaQlim is interdisciplinary (geology, geophysics, geodesy, seismology), it has global relevance and potentially wide geographic coverage, and it will provide new results in basic geosciences. On the geodetic side, the benefit of the multi-disciplinary approach is the improved crustal dynamics models which will be used for precise and stable global reference frames, essential in the coming decades. And vice versa, geodetic techniques and stable reference frames are needed in this research.

As a result of the DynaQlim project we expect to have a more comprehensive understanding of the Earth's response to glaciations, improved modelling of crustal and upper mantle dynamics as rheology structure. An important aspect is to construct and improve coupled models of glaciation and land-uplift history and their connection to the climate evolution on the time scale of glacial cycles. Results can be applied for the contemporary climate evolution, consequences of the global change and fate and future of the current glaciers (Poutanen et al. 2009).

On the local level, participation in the *GeoSatakunta* project under the aforementioned framework allows us to study both land uplift and local geodynamics in a detailed way. This far, GeoSatakunta project (in 2008-2009, InnoGeo) has been funded by EU, Cities of Pori and Rauma, Posiva Ltd and participating institutes. The main participants in the research are the Geological Survey of Finland, the Finnish Geodetic Institute (FGI), and the City of Pori.

A network of 13 GPS points has been established in the area in 2002-2006, and the FGI is performing regular measurements three times per year as described in the next chapter. A sub-network around the Olkiluoto nuclear power station has been monitored already more than a decade. The Olkiluoto network is nowadays connected to the larger GeoSatakunta network.

Partly funded by the Academy of Finland, the FGI is performing a study on precise geoid models in the area. Geoid will give additional information, as one can see in Figure 1-1.



### 3 GPS OBSERVING ERRORS

GPS is an excellent tool for deformation studies. There is no need for inter-station visibility, distances are not limited to the local scale and accuracies are generally superb to the traditional methods, especially over longer distances. There are, however, some limitations in accuracy due to observation errors. Especially heights and height changes are more difficult to monitor with GPS than the horizontal motions. Some of the GPS errors are random, and can be minimized by increasing the number of observations or length of time series. Others can be more systematic, and in those cases biases cannot be removed. However, in most cases we may assume that biases are constant in time and therefore cancelled if we are monitoring only changes.

During the post-processing, software normally gives also estimation on the accuracy. In many cases the formal errors of a GPS solution do not agree with the actual errors of the measurement but are normally far too optimistic. This indicates that the error distribution does not obey white noise or there are unresolved biases. Repeatability of observations is a better indication of accuracy.

In the following we discuss some of the errors in GPS deformation studies and how they affect the accuracy. The error sources include the satellite orbit errors (Figure 3-1), ionosphere and troposphere refraction, multipath and antenna electric phase centre variation.

Currently, orbital accuracy based on Broadcast ephemeris of GPS satellites is in the range of 1-2 meters and clock errors smaller than 10 ns (IGS, 2008). With IGS precise ephemeris one can get down to 0.05 m and 0.1 ns, respectively. In most precise deformation studies precise orbits are recommended, although errors due to the broadcast ephemeris will remain well below 0.1 ppm. In our work we have used IGS precise orbits and clocks for satellites.

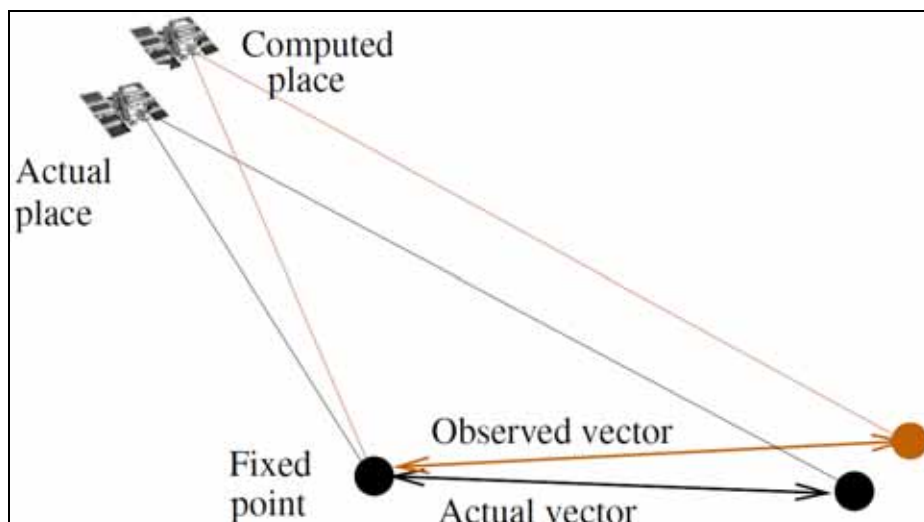


**Figure 3-1.** Effect of the satellite orbit error on observed vectors. As a rule of thumb, 25 m error in satellite orbit cause 1 ppm error in observed position. Currently, satellite broadcast ephemeris are better than 2.5 m, and precise ephemeris better than 0.05 m. In most cases orbit-related errors are insignificant.

There are three major sources of error in the signal propagation from the satellite to the receiver. These are ionosphere, troposphere and multipath. In the GPS terminology, we divide the medium between the satellite and receiver in two parts: the neutral part of the atmosphere, below 50-60 km is called troposphere, and the rest (above some 60 km) is called ionosphere. Both cause signal delay and change in apparent observed distance to the satellite. This is sometimes called ionosphere and troposphere refraction.

Ionosphere is dispersive and the signal propagation depends on its frequency. Therefore it is possible to eliminate the ionosphere in dual frequency observations where an ionosphere-free combination can be created. Troposphere is non-dispersive in GPS frequencies, and therefore it is not possible to eliminate in the same way. Multipath depends on the surroundings of the antenna and is unique for each site and time. It is caused by reflections of the signal from various surfaces around the antenna causing the signal to come to the antenna from several paths.

A simplified observation equation for the carrier pseudorange  $L_i$  (the observed distance using the carrier wavelength, and which is corrupted by several sources of errors) in the frequency  $i$  can be written as

$$L_i = (N + \varphi)\lambda + c \cdot \delta T + \Delta_i^{ion} + \Delta_i^{trop} + \Delta_i^{multi} + \dots$$

where  $N$  is the number of full carrier wavelengths between the satellite and the receiver,  $\varphi$  is the fractional part,  $\lambda$  is the wavelength,  $c$  is the speed of light,  $\delta T$  is the clock error, and  $\Delta$ 's are the ionosphere, troposphere and multipath effect on the signal in frequency  $i$ . The true distance is  $(N + \varphi)\lambda$ .

The effect of the ionosphere is inversely proportional to the square of the frequency  $f$  and directly proportional to TEC, the total number of free electrons in the signal path

$$\Delta_i^{ion} \propto \text{TEC} / f_i^2.$$

If we denote the observed pseudorange in frequency  $f_1$  by  $L_1$  and pseudorange in  $f_2$  by  $L_2$  we can write the ionosphere-free combination  $L_3$  as follows (Dach et al. 2007)

$$L_3 = \frac{f_{L1}^2}{f_{L1}^2 - f_{L2}^2} L_1 - \frac{f_{L2}^2}{f_{L1}^2 - f_{L2}^2} L_2.$$

This virtually eliminates the effect of the ionosphere in observations but the noise is increased by a factor of 3. Therefore ionosphere-free combination is used only in long vectors (longer than 15-20 km). An alternative is to create an ionosphere model.

The ionosphere model can be made using the local observations and creating the geometry-free combination  $L_4$ ,

$$L_4 = L_1 - L_2.$$

$L_4$  is independent of receiver clocks, satellite clocks, orbits or station coordinates, and it only contains the ionospheric delay.

The local model is often expressed as (Dach et al. 2007)

$$E(\varphi, \lambda) = \sum_{n=0}^{n_{\max}} \sum_{m=0}^{m_{\max}} E_{nm} (\varphi - \varphi_0)^n (\lambda - \lambda_0)^m$$

where

$n_{\max}, m_{\max}$  are the maximum degrees of the Taylor expansion in latitude  $\varphi$  and longitude  $\lambda$ ,

$E_{nm}$  are the local ionosphere model parameters to be estimated, and

$\varphi_0, \lambda_0$  are the coordinates of the origin of the development.

We have noticed that GPS solutions may be significantly biased by scale errors (Ollikainen & Kakkuri 1999). This systematic scale error is mainly caused by the ionosphere. The scale error has varied from -0.8 to +0.6 ppm at Oulkuu. However in 2002 measurements at Romuvaara in NE Finland it was as large as +2.1 ppm. This is due because the ionosphere will change the apparent path of the signal in much shorter time scales than what is possible to apply in the ionospheric models.

In the Oulkuu network local ionosphere models have been used. However, in the GeoSatakunta network we have chosen a different approach using the Quasi-ionosphere free model QIF (Dach et al. 2007). This allows us the integer ambiguity resolution on the double difference level in the final computation.

Troposphere related errors are more difficult to eliminate than the ionosphere errors because troposphere affects in the same way in L1 and L2 frequencies. The troposphere is a non-dispersive medium for radio waves up to frequencies of about 15 GHz and therefore tropospheric refraction is identical for L1 and L2 carriers. The effect of the troposphere depends on the refractive index of the air which is a function of the pressure, temperature and humidity. Quite often the troposphere refraction is divided into two parts, “dry” and “wet”,

$$\Delta^{trop} = \Delta^{dry} + \Delta^{wet},$$

where the hydrostatic part (“dry”) consists of about 90 % of the total delay. The effect of the water vapour is extremely variable and it cannot be modeled as the hydrostatic part. Measurement of the water vapour content via the signal path is not possible in routine measurement. Use of a standard troposphere model may result in an error which affects both scale and height.

The scale error  $\Delta l / l$  is (Dach et al. 2007)

$$\frac{\Delta l}{l} = \frac{\Delta \rho}{R_{\oplus} \cos z_{\max}}$$

where  $\Delta \rho$  is the troposphere model error,  $R_{\oplus}$  is the Earth's radius and  $z_{\max}$  is the maximum observed zenith angle. The height error  $\Delta h$  between points  $a$  and  $b$  amounts to

$$\Delta h = \delta \Delta \rho_{ab} / \cos z_{\max}$$

where  $\delta \Delta \rho_{ab}$  is the relative troposphere error between points  $a$  and  $b$ .

Troposphere error grows rapidly at small elevation angles (Figure 3-2). Therefore, in many applications the cut-off limit in GPS processing is set to  $15^\circ$  below which the observations are not used. In addition of the troposphere model, we use in our computation an elevation-dependent unknown on each site to estimate the residual part of the tropospheric refraction after subtraction of a standard model value.

Multipath is caused by signal entering the antenna from more than one route. Reflections from water, roofs and other nearby structures cause an error, the size of which is only in centimetre range but can easily destroy deformation measurements where sub-centimetre accuracies are needed. For every site (or even for every antenna installation) the multipath is unique, it is highly time dependent, and it cannot be eliminated with modelling. It can be minimized by using a special type of antenna structure, so called choke ring antennas, where the antenna element is installed in the centre of co-centric rings (Figure 3-3). This kind of antenna structure is nowadays a *de facto* standard in precise GPS measurements. Another way to minimize the effect is to observe 24 h sessions to get all possible multipath values. In our observations we use Ashtech Dorne Margolin type choke ring antennas and 24 h observing sessions.

Antenna phase centre variation is one of the remarkable sources of error. The position of the antenna electrical phase centre depends e.g. on the direction and frequency of the incoming signal. If identical antennae are used in the whole network, the phase centre error cancels out almost totally but if there are different antennae (or even different antenna mounting, radome, snow on top of an antenna, multipath...), the error remains. The phase centre variation causes a systematic error in height which cannot necessarily be seen in normal processing, although it can be even centimetres. It can be eliminated with a field calibration but this implies a lot of extra work. Another method is to use calibration tables which exist for each antenna type and can be used with advanced GPS processing software. We minimize the phase centre variation by using identical antennas, mounting the same antenna every time on the same site, using the 24 h observing sessions to get an average over all possible phase centre positions, and using individually and absolutely calibrated antenna correction tables in post processing software.

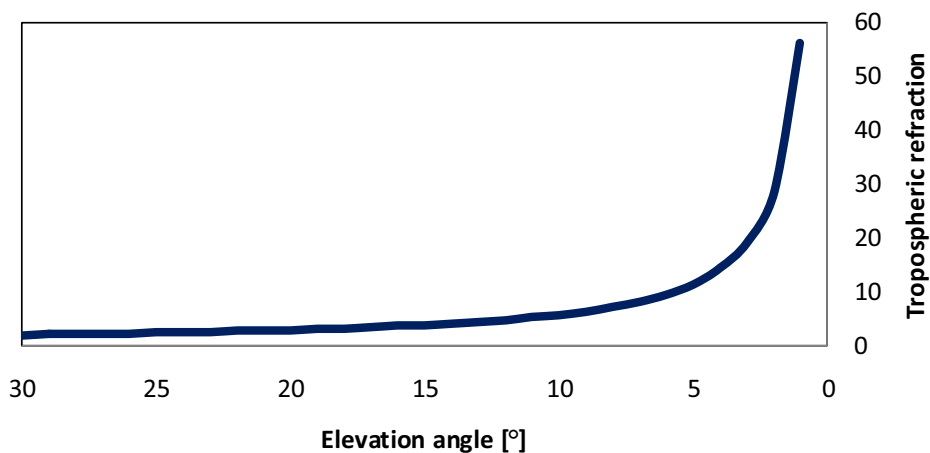


**Figure 3-2.** The effect of tropospheric refraction as a function of the satellite elevation angle.



**Figure 3-3.** Dorne Margolin type choke ring antenna. This kind of structure damps the effect of multipath. The antenna type is a de facto standard in precise GPS measurements. (Photograph M. Poutanen)



## **4 GEOSATAKUNTA GPS NETWORK AND MEASUREMENTS**

### **4.1 Network planning and site selection**

One of the goals of the GeoSatakunta project is to obtain information about possible crustal deformations in the area. Accurate GPS-measurements are most suitable to determine horizontal movements over a large area.

There are several criteria which must be fulfilled when selecting the sites. First of all, observation sites must be open so that signals from satellites can be received. Because we will make measurements during many years, naturally open places are better than manmade openings in a forest. For the same reason, the benchmarks (or pillars in this case) have to be established into solid bedrock. Permissions for the pillars from land owners set additional constraints to the network. Finally, the shape of the GPS network must be geometrically reasonable.

In our case, we had also other constraints, concerning the geological structure of the area. The goal was to establish the sites on different geological structures connecting the Jotnian sandstone, Postjotnian diabase and the Rapakivi granite areas. We also wanted to have sites on both sides of the Kynsikangas shear zone complex.

Geological Survey of Finland chose places for site candidates using their geological knowledge about the Satakunta area. Based on this geological selection, the city surveyors of the City of Pori made the reconnaissance for the final sites and they also made the agreements with land owners. City of Pori has been an active member of the GeoSatakunta project already from the very beginning. They planned to use the pillars and observations also for their own purposes. Such a network would serve municipalities in the area as an excellent reference network in local surveys.

First seven pillars (numbers 1-7, see Figure 4-1) were built in November 2002 in the vicinity of the City of Pori. First measurement campaign was already in January 2003. Olkiluoto permanent FinnRef<sup>®</sup> GPS station was included in the original network, too.

After a few years the City of Rauma joined the GeoSatakunta project. At the same time Posiva proposed to connect their deformation studies of Olkiluoto to the GeoSatakunta investigations. Therefore, new pillars GPS14, GPS15 and 9 were established in October 2005. Pillar 10 was established in April 2006 and pillar 8 in October 2006. Pillars GPS11 and GPS12 in the Posiva network were built in August 2003. Only pillar GPS11 has been used in GeoSatakunta measurements (Table 4-1).

### **4.2 GPS pillars**

The Cities of Pori and Rauma constructed the GPS pillars which are made of reinforced concrete on-site (Figure 4-2 and 4-3). An attachment into solid bedrock has been made with iron bars. Concrete was carried from the nearest road to the site which gave its own constraint to the size and placement of the pillar. Photographs of all pillars are presented in Figure 4-7.



**Figure 4-1.** GeoSatakunta GPS network. Base map © National Land Survey, license number 51/MML/09.

An antenna platform was installed on the top of pillar at the same time the pillar was casted (Figure 4-4 and 4-5). The platform is made of stainless steel with a  $\frac{3}{4}$  inch hole in the middle to use a standard-sized screw for the antenna. There are no adjustments possible after casting, when the platform was set in level.

There are some advantages of the simple structure. Because the antenna is directly attached to the platform without any interface or forced centering device, its height and position is preserved between campaigns. There is no need to make additional centering measurements, and different observers with various equipments will have their reference always to the same point. Moreover, open and simple structure will not attract vandals when the pillar is unattended.

**Table 4-1.** Approximate coordinates of GeoSatakunta GPS network in EUREF-FIN and the year of establishment.

Site	Name	X [m]	Y [m]	Z [m]	Year
OLKI	Olkiluoto	2863210.3	1126271.4	5568267.2	1994
1	Tahkoluoto	2829486.2	1107559.1	5589070.2	2002
2	Kivini	2830882.5	1126749.7	5584556.3	2002
3	Peräkulma	2842896.0	1129969.3	5577889.5	2002
4	Kuorila	2833450.6	1143091.4	5579998.0	2002
5	Nakkila	2839303.6	1151482.8	5575328.5	2002
6	Sääksjärvi	2822310.9	1147666.2	5584713.1	2002
7	Järventausta	2825465.2	1162441.2	5580109.9	2002
8	Huikko	2852909.1	1151451.6	5568442.8	2006
9	Monna	2874084.3	1135529.6	5560850.6	2005
10	Virovuori	2867232.3	1152070.6	5561012.2	2006
GPS11	Kuivalahti	2859164.5	1133699.2	5568849.4	2003
GPS14	Hankkila	2864514.9	1133711.2	5566120.9	2005
GPS15	Taipalmaa	2866984.1	1129664.5	5565663.1	2005



**Figure 4-2.** City of Pori surveyors have been built most of the observation pillars. (Photograph J. Ahola.)

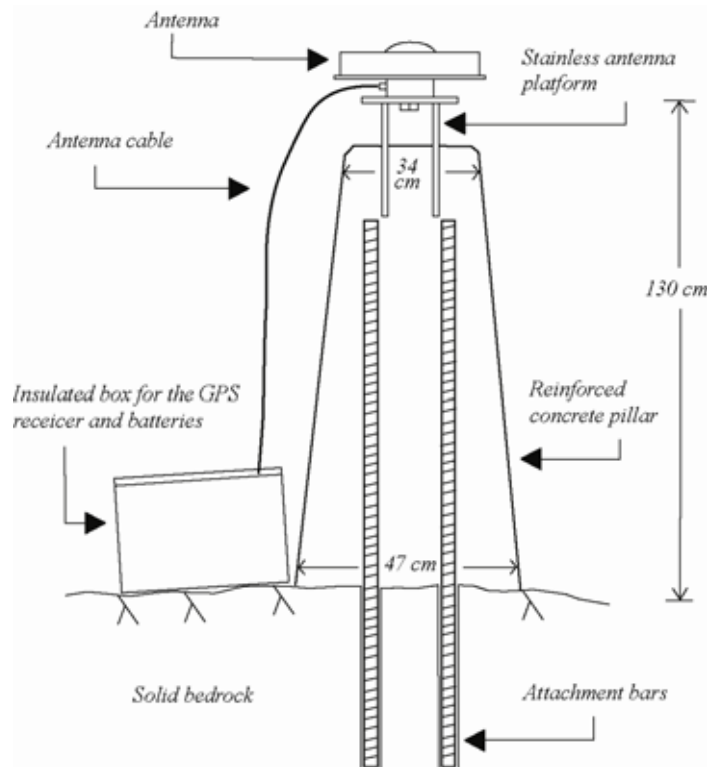


**Figure 4-3.** Construction of GPS pillar.



**Figure 4-4.** A proper position of the antenna platform is measured with a builder's level when the pillar was casted. After that the platform cannot be adjusted. (Photograph J. Ahola.)



*Figure 4-5. A Dorne Margolin type antenna on a pillar. (Photograph J. Ahola.)*



*Figure 4-6. Receiver and batteries in the instrument box. (Photograph J. Ahola.)*



a)



b)



c)



d)

**Figure 4-7.** a) 1 Tahkoluoto is an open site near the shoreline. b) 2 Kivini is on the natural protection area and there are few trees around the pillar. c) 3 Peräkulma is located in a large forest cutting area which will be open at least next 15 years. d) 4 Kuorila is on the top of an open hill.



e)



f)



g)



h)

**Figure 4-7. (continued)** e) 5 Nakkila has been built near an old cow shelter which causes deterioration of the signal. The site is not suitable for high-precision deformation measurements. f) 6 Sääksjärvi is located in a small forest cutting area. g) 7 Järventausta has been established on the top of a rocky hill. h) 8 Huikko is located near the crossroad.



i)



j)



k)



l)

**Figure 4-7. (continued)** i) 9 Monna has been built under an electric line. j) 10 Virovuori is located on an open rocky hill. k) GSP11 Kuivalahti has been built on the top of a hill. It is a part of Olkiluoto local network and there is an absolute gravity point at the same site. l) GPS14 Hankkila has been established under an electric line.



m)



n)



o)

**Figure 4-7. (continued)** m) GPS15 Taipalmaa is located on top of a naturally open hill. n) OLKI Olkiluoto is a permanent GPS station of the FinnRef<sup>®</sup> network. Photograph has been taken in 2003. After that the surrounding pine trees have grown 3 to 5 meter tall. o) GPS12 Iso Pyrekari is located on a small islet. It belongs to the Olkiluoto local network, but we have not measured it in GeoSatakunta campaigns because of transportation problems there. (Photographs J. Ahola.)

### 4.3 Control markers

All the pillars are attached to the solid bedrock. We expect that the pillars are stable and the possible movements we observe are due to deformation. However, we cannot exclude the possibility of an unexpected event which may destroy the antenna platform or cause some damage to the pillar. Therefore we established auxiliary markers at pillars in 2006. The City of Pori assisted in the field work in 2006 when three markers were placed in the vicinity of each pillar. At the point 5 Nakkila it was not possible to establish auxiliary markers.

The centering measurements were made in 2006 with a precise tacheometer Wild T2002+DI2002. At the same time, azimuth from the pillar to the markers was determined using two GPS receivers. We are able to control the stability of the pillars by repeated centering measurements. The measurement accuracy is some tenths of millimeters which is enough to ensure the stability of the pillar. However, in this network accuracies are so high that the reconstruction of a destroyed pillar is not possible.



*Figure 4-8. Establishment of an auxiliary marker. (Photograph J. Ahola)*



*Figure 4-9. Centering measurement of the pillar at Tahkoluoto. (Photograph J. Ahola)*

#### **4.4 Equipments and measurement campaigns**

Measurement campaigns have been done in a co-operation with the Cities of Pori and (since 2005) Rauma. City of Pori has offered personnel and a car in transportation to the sites. We have observed the network three times per year since January 2003. First measurement has been in February, the second one in June and the last one in the middle of October (Table 4-2). The temperature has been varied from  $-25\text{ }^{\circ}\text{C}$  to  $+25\text{ }^{\circ}\text{C}$  and the weather from sunshine to heavy rain.

The receiver and batteries are in an insulated box during the measurements (Fig. 4-6). The thermal insulation is necessary during the winter observations when the temperature can be well below zero. The box is attached with a chain and padlock to the pillar.

We have used Ashtech Z12 and  $\mu\text{Z}$  dual frequency receivers of the Finnish Geodetic Institute for the field campaigns. In all campaigns Ashtech Dorne Margolin Choke Ring antennas were attached directly on the platform using special bolts which fit perfectly on the hole of the platform. This eliminates centering and adjustment errors. Moreover, we ensured that the same antenna was used on the same pillar every time to eliminate the individual antenna phase center errors (Table 4-3).

Table 4-2. Schedule of the GPS campaigns.

Campaign	Time	Observed sites														
		1	2	3	4	5	6	7	8	9	10	11	14	15	OLKI	
2003-1	21.-25.1.	X	X	X	X	X	X	X								X
2003-2	2.-3.6.	X	X	X	X	X	X	X								X
2003-3	20.-21.10.	X	X	X	X	X	X	X								X
2004-1	10.-11.2.	X	X	X	X	X	X	X								X
2004-2	8.-9.2.	X	X	X	X	X	X	X								X
2004-3	20.-21.10.	X	X	X	X	X	X	X								X
2005-1	8.-9.2.	X	X	X	X	X	X	X								X
2005-2	1.-2.6.	X	X	X	X	X	X	X								X
2005-3	17.-20.10	X	X	X	X	X	X	X		X		X	X	X		X
2006-1	6.-9.2.	X	X	X	X	X	X	X		X		X	X	X		X
2006-2	29.5.-1.6.	X	X	X	X	X	X	X		X	X	X	X	X		X
2006-3	23.-26.10.	X	X	X	X	X	X	X	X	X	X	X	X	X		X
2007-1	5.-8.2.	X	X	X	X	X	X	X	X	X	X	X	X	X		X
2007-2	4.-7.6.	X	X	X	X	X	X	X	X	X	X	X	X	X		X
2007-3	15.-18.10.	X	X	X	X	X	X	X	X	X	X	X	X	X		X
2008-1	11.-14.2.	X	X	X	X	X	X	X	X	X	X	X	X	X		X
2008-2	2.-5.6.	X	X	X	X	X	X	X	X	X	X	X	X	X		X
2008-3	3.-6.11.	X	X	X	X	X	X	X	X	X	X	X	X	X		X

Table 4-3. Receivers and antennas used in campaigns.

Station	1	2	3	4	5	6	7	8	9	10	OL11	OL14	OL15	Olkiluoto
1-2003	03398	03436	04300	04293	LP00164U	03398	03436							03176
2-2003	03398	03436	LP00164U	GP10273	04293	LP00106U	04300							03176
3-2003	LP00174	04108	03436	03398	LP00168	LP00164U	GP10273							03176
1-2004	03398	04104	LP00164U	04098	LP00168	LP00174	GP10273							03176
2-2004	03398	LP00174	04098	LP00168	GP10273	LP00164U	03175							03176
3-2004	03176	04293	GP10273	03436	LP01087	ZR20001907	04098							LP00168
1-2005	03176	04293	LP00106U	03436	LP01087	ZR20001907	04098							LP00168
2-2005	LP00106U	04293	03176	04098	LP00164U	03436	LP01087							LP00168
3-2005	04300	04108	ZR20000701	ZR20001907	03398	LP01087	LP00164U		LP01087		04300	04108	LP00164U	LP00168
1-2006	04293	03436	ZR20000701	ZR20001907	03398	04300	LP00164U		04300		04293	04108	LP00164U	LP00168
2-2006	03436	LP00164U	LP01087	ZR20001907	04098	04108	04300		04108	04098	03436	LP00164U	04300	LP00168
3-2006	04098	03398	LP00174	ZR20000701	04293	LP01087	LP00164U	ZR2001907	LP01087	04293	04098	03398	LP00164U	LP00168
1-2007	04098	03398	ZR20001907	ZR20000701	LP00184U	LP01087	LP00164U	LP00174	LP01087	LP00184U	04098	03398	LP00164U	LP00168
2-2007	04293	04098	ZR20000701	ZR20001907	LP00164U	LP00167U	LP00184U	LP00174	04293	04098	LP00164U	LP00184U	LP00167U	LP00168
3-2007	03175	04098	LP00167U	ZR20000701	LP00184U	04293	GP10273	LP00164U	04293	03175	LP00184U	GP10273	04098	LP00168
1-2008	03175	04098	LP00167U	GP10273	LP00184U	04293	04108	LP00164U	04293	03175	LP00184U	04108	04098	LP00168
2-2008	LP02547	04293	LP00134U	GP10273	LP00167U	04300	04098	LP00164U	LP02547	04293	LP00167U	04098	04300	LP00168
3-2008	03398	04300	LP00167U	GP10273	LP02547	04098	LP00164U	LP00164U	LP02547	LP00184U	03398	04098	04300	LP00168
Antenna	11754	11772	11770	11761	11963	11959	11988	11194	11959	11963	11754	11772	11988	321
Exceptions				CR13995 (1-2003)		11754 (1-2003), 11194 (1-2004)	11772 (1-2003)							

In 2003-2005/2 observations were taken in one session lasting 24 hours. After the extension of the network, there were too many pillars to cover all of them in one session. Therefore, the total time for the field work increased from two days to four and the receivers were moved to the new pillars between the sessions.

With 24 hour-long sessions we try to diminish or eliminate satellite geometry and signal multipath related errors. During the 24 hour session the satellite geometry is changing to all possible states. Also the multipath repeats itself after one sidereal day, and therefore no new information is obtained after that. As a first approximation, multipath can be considered as a random error in a 24-h session.

Observations are taken in 30 s interval, using  $5^\circ$  cut-off angle. Due to the local circumstances, visibility is not free down to the horizon but obstacles like trees and buildings limit the visibility in some directions to much higher angles. Also the signal noise and multipath are increased with the zenith angle. Therefore, in processing the actual cut-off angle is much higher,  $15^\circ$  but all observations are archived for possible future use.



## 5 COMPUTATION

### 5.1 Computation software and strategy

The preliminary computation was made with *Trimble Total Control* (TTC) software. This was a “quick-check” to ensure that measurements were successful. This gives also the first estimation about the accuracy of the measurement and reveals possible problematic data.

Final computation, presented here, was done using Bernese v.5.0 software (Dach *et al.* 2007). This software is meant for scientific processing and it is widely used for similar high-precision networks ranging from global to local. The user has a possibility to define the processing parameters in full detail, but at the same time the processing is very demanding and time-consuming compared to commercial software. Because the user has a full control over the processing parameters, and he can choose best possible strategy, results are more accurate and variation is smaller. To process all campaigns in reasonable time the computation process was automated using the Bernese Processing Engine. The automation also enabled fast repeat of processing for determining the best possible processing strategy and parameters.

We have used IGS precise orbital elements to minimize satellite orbit related errors. Broadcast elements may give rise of up to 0.1 ppm errors in computed vectors which amount up to millimeter-range errors over longest vectors.

Observations were taken down to  $5^\circ$  but in processing we used  $15^\circ$  cut-off angle. There are several reasons for this; most importantly that on many sites visibility below  $15^\circ$  is restricted by trees and buildings. Also multipath, and ionospheric and tropospheric disturbances are increasing rapidly with smaller elevation angles. In practice,  $15^\circ$ – $20^\circ$  cut-off angle has turned out to be a reasonable compromise between data loss and avoiding low elevation related errors.

The data processing strategy was developed according to the general rules of GPS-processing with a special attention to outlier detection. The vector lengths range from five to 65 km. This set some further demands on the processing strategy. For shortest vectors, L1 (or L1 and L2 separately) gives best results, but when the length is well above 10 km, an ionosphere correction needs to be applied.

Single vectors were resolved in three stages. First we used L3 ionosphere-free linear combination for data screening and outlier detection to eliminate the large scattering detected in preliminary computation (Poutanen and Ahola, 2010). After that we used a Quasi-ionosphere free combination (QIF) of the Bernese software (Dach *et al.* 2007). This is formed combining L1 and L2 in a way where the integer character of the signal carrier wavelength is preserved on the double difference level. This improves stability and accuracy of the solution. The final solution was estimated using L3 and resolved ambiguities.

Single vectors between individual pillars were computed in one session. After that a network adjustment was applied where the Olkiluoto permanent station was kept fixed. As a result we obtain coordinates of the pillars.

## 5.2. GPS processing results

The GPS processing results showed that the computation was carried out successfully. The rms-values in the different parts of the computation process lied within the desired limits and the scattering of the results between different sessions was small. However, few problematic sessions and observations sites (pillars) were detected.

The effect of the processing strategy is clearly visible in the vector solutions. The figure 5-1 clearly shows the importance of the residual screening and outlier detection before final vector solutions. The vector rms-values of the campaign 2004-3 were larger than in other sessions when processed without residual analysis.

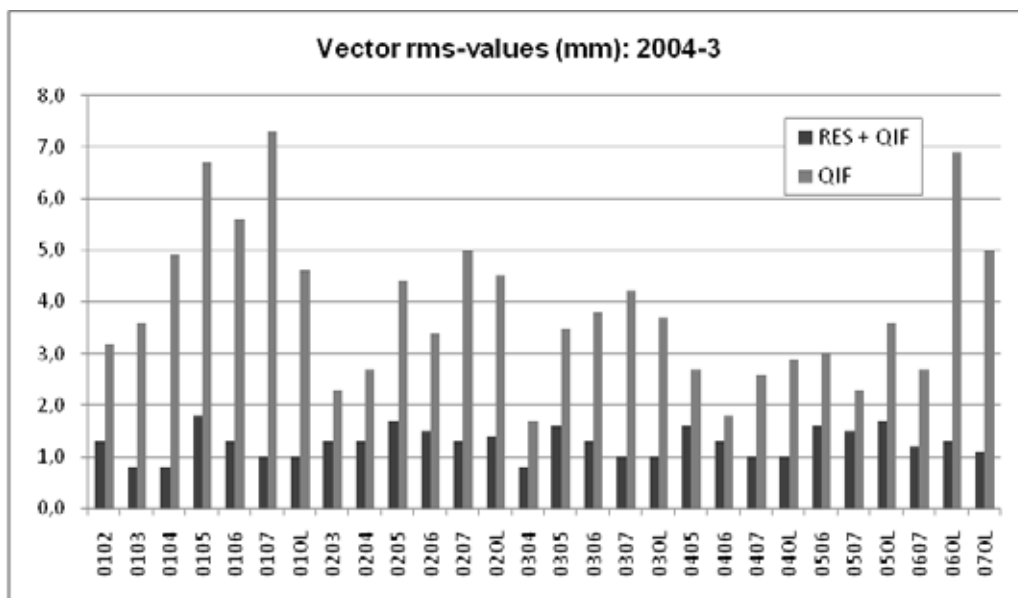


**Figure 5-1.** Large rms values were detected in vector solutions in the 2004-3 campaign if processed by QIF-strategy only. After the residual screening (RES+QIF) the rms values are of the same order of magnitude as in other sessions.

Typical rms-values of a vector solution are shown in figures 5-2 and 5-3. The residual analysis does not affect on the best resolved vectors (smallest rms-values) but generally it improves slightly the solutions. The rms-values of individual vectors in different sessions scatter only some tenths of millimetres. In the second session (figure 5-3) there were a lot of short and well-resolved vectors but the pillar 8 (Huikko) stands out clearly. After the residual analysis it has still the largest rms-values of the session but now they are of the same order of magnitude as the other vectors in the first session. In the final solution the vector rms-values varied from 0.5-1.6 mm without any significant scattering.

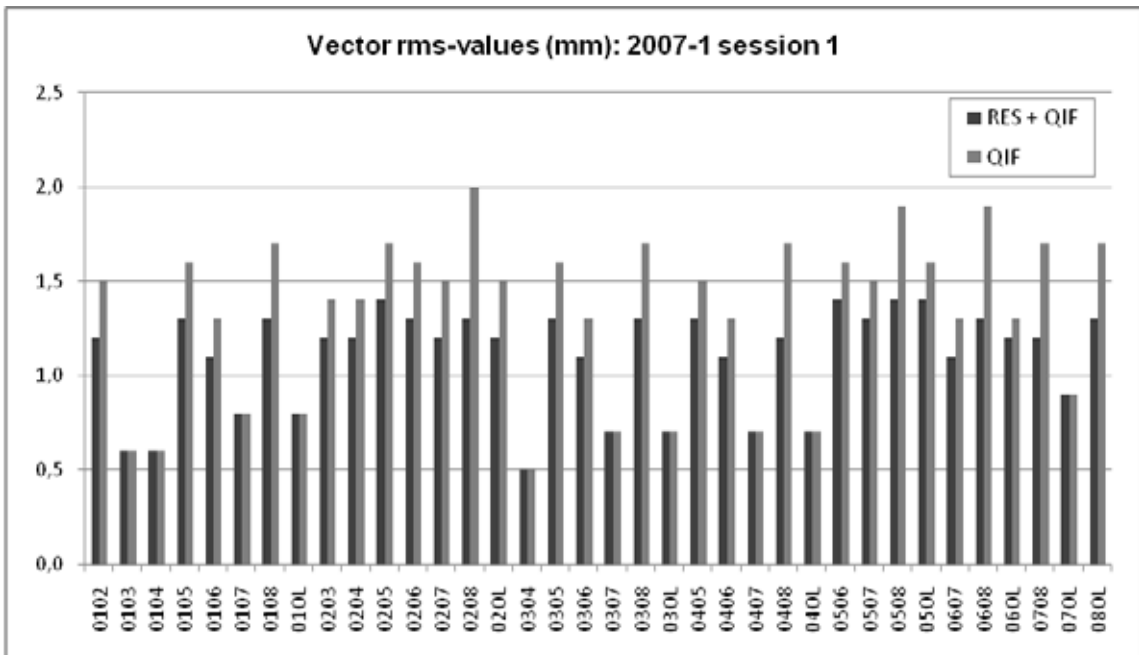


**Figure 5-2.** Automated residual analysis improves the accuracy of vector solutions.

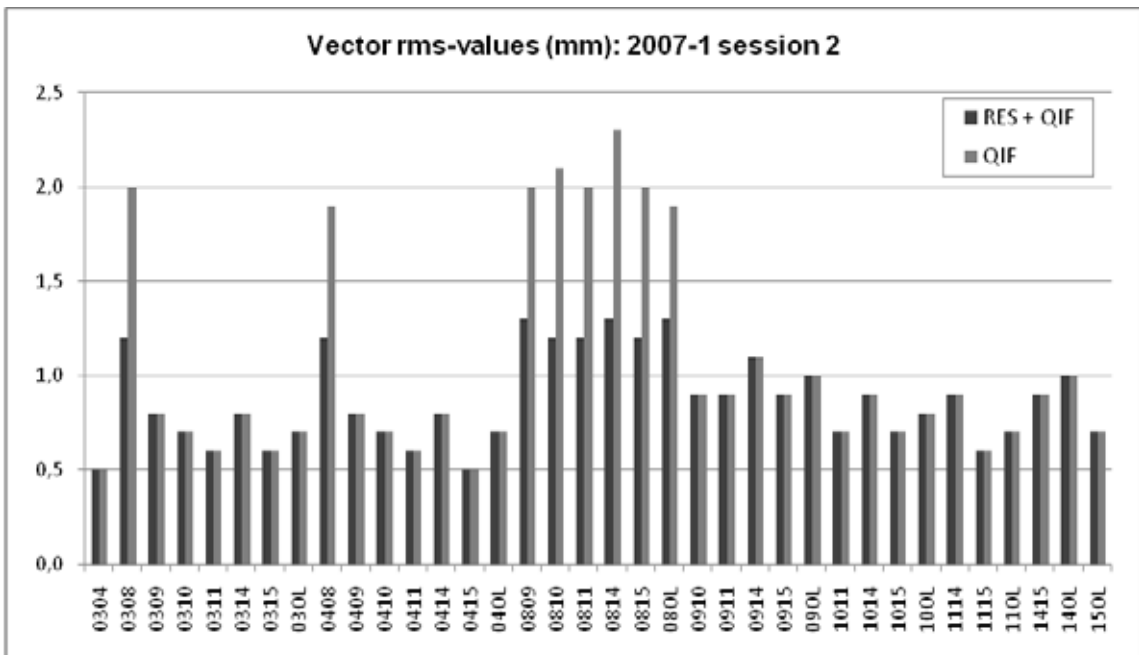


**Figure 5-3.** In the second session there were a lot of short and well-resolved vectors but the pillar 8 is problematic: it has the largest rms-values also after the residual screening.



## 6 DATA ANALYSIS

GPS processing results of single session give good indication of data quality and reliability of the solution. However, the scattering in the vector time series can be large due to the character of GPS-observations. This makes the deformation analysis challenging. To determine the deformation of the network we analysed the vector time series and estimated the velocities of the pillars.

### 6.1 Vector time series

Using vector lengths computed from the coordinates of the pillars (Appendix 1), we can plot time series of the vectors in the network. The main features of plots are displayed here and a larger set of time series are shown in Appendix 2. The results of the preliminary computation (Poutanen & Ahola 2010) are included in plots to analyse and compare the solutions.

The scattering in the vector time series is on average less than 2.0 mm and mainly smaller than in Ahola's computation. Vectors with largest rms-values have also the largest scattering in time series plots and vice versa. The session-to-session scattering is expected but the difference between a good and problematic site is clear (Figures 6-1 and 6-2). The large scattering on sites 5 (Nakkila) and 8 (Huikko) is mainly because of obstacles are limiting the visibility at the site.

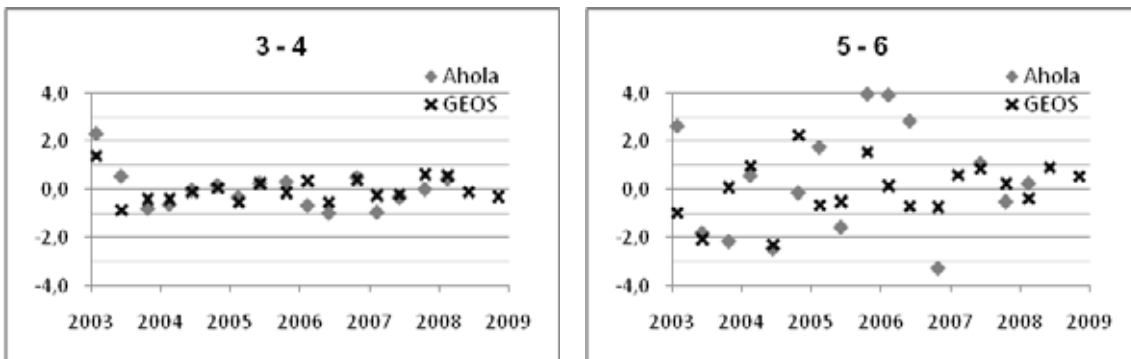


**Figure 6-1.** Example of a good and a problematic site (deviation from mean (mm)). In the case of problematic vector (5–6) the scattering is smaller in this determination (GEOS) compared with preliminary computation (Ahola).

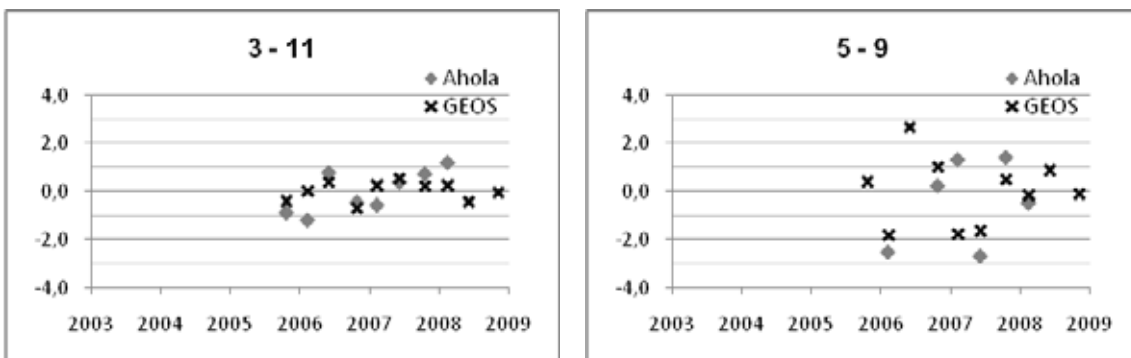


**Figure 6-2.** Short time series behave very similar to longer ones.

As already showed in the vector solution, the effect of the computation strategy is obvious in case of problematic sites whereas the time series are nearly identical in case of a good site. With the processing strategy used in this research we could eliminate most of the outliers existed in the preliminary computation (Figure 6-3). However, few outliers still exists in time series. The final L3 solution in vector processing did not improve rms-values of the solution, but a positive smoothing effect can be seen in some of the time series plots (Figure 6-4). In the final solution only the first observation (campaign 2003-1) seems to be an outlier and others the scattering is smaller than after QIF-solution.

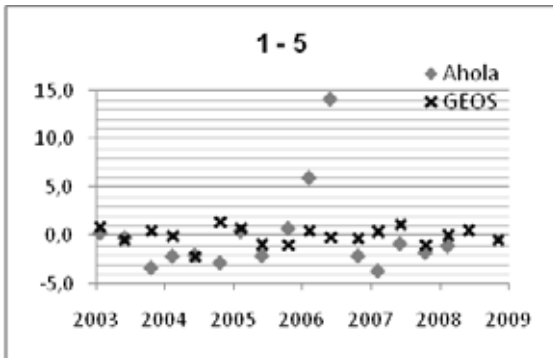


**Figure 6-3.** The outliers of the preliminary computation have disappeared in this solution.

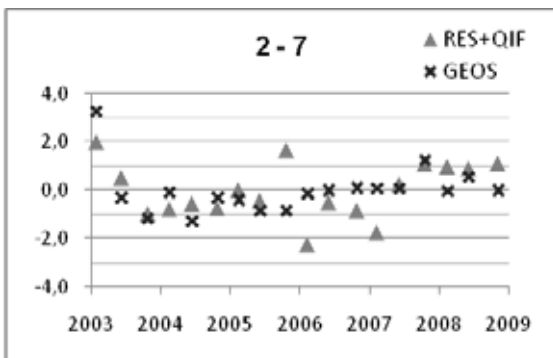


**Figure 6-4.** The final L3 solution (GEOS) still improves a bit the fairly good QIF-solution.

When analysing standard deviation of the time series as a function of vector length, there are no outlying observations and the small distance dependency is expected (Figure 6-5). Thus, any of the observation sites is not significantly more uncertain than others which would be seen in the figure. Figure 6-6 demonstrates the character of GPS-measurements. The time series from a single station behave uniformly. The measurement conditions are unique in every session and affect a lot to the received signals. Therefore a well resolved vector might, however, behave like an outlier in time series analysis. The detected behaviour is partly due to the uniform processing of the data.

The time series analysis showed that the GPS processing was successful. There was no evident trend in time series. Mostly the scattering was relatively large compared to the potential movement and hence, it is not possible to confirm any deformation. There are, however, some vectors with small scattering (less than 1.0 mm) with signs of minor changes.

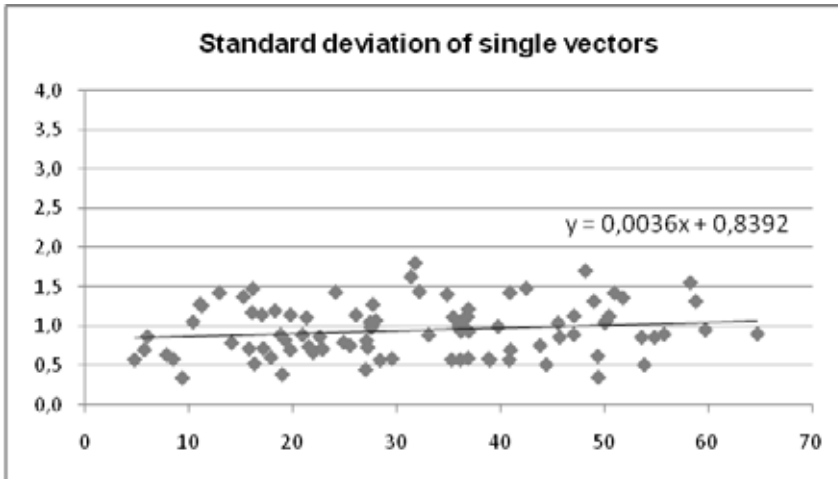


**Figure 6-5.** Standard deviation (mm) as a function of vector length (km). Deviation depends only slightly on the vector length.

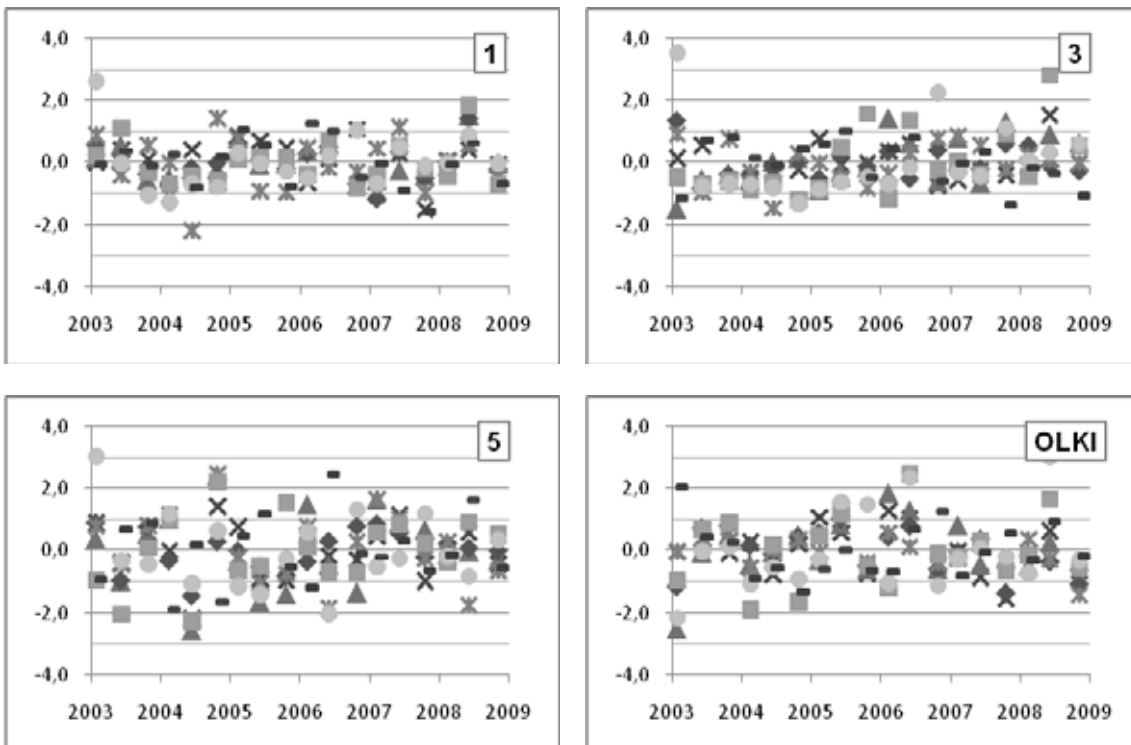


**Figure 6-6.** Vector time series from points 1, 3, 5 and OLKI. There seems to be some common trends. The larger scattering of the pillar 5 is mainly due to obstacles limiting the visibility at site.

## 6.2 Deformation analysis

To get the first approximation of the crustal movements and to determine the velocities of the pillars we performed a deformation analysis (Kallio et al. 2009a) using coordinate time series. The deformation analysis was based on the coordinate differences between adjacent pillars and the Delaunay-triangulation was used. A free network adjustment was applied with station specific velocity parameters ( $v_x, v_y, v_z$ ) as additional parameters. The resolved velocities were transformed to the North-East-Up system. To illustrate the horizontal movements, the station velocities were interpolated in a grid and visualized as a velocity vector map. The results of the deformation analysis are presented in Table 6-1 and Figure 6-7. We used  $3\sigma$  as a limit to test the statistical significance of the estimated velocities: we consider the velocity significant if it is three times larger than the mean error.

The results show that only the north component of the pillar 6 (Sääksjärvi) is statistically significant. The larger mean errors of the southern part of the network are because of the shorter time series. Hence the estimated velocities, especially for the southern part of the network, are quite uncertain. The uncertainty of the results can be observed also when running the deformation analysis using the QIF-solution, which was nearly as good as the final solution. Then the magnitudes and directions of the velocity vectors vary in some parts of the network clearly.

**Table 6-1.** Results of the deformation analysis, statistically significant velocities in bold.

	Velocity (mm/a)		Mean error (mm/a)	
	North	East	North	East
<b>1</b>	-0,10	0,03	0,08	0,06
<b>2</b>	0,12	0,11	0,08	0,06
<b>3</b>	-0,13	0,03	0,07	0,05
<b>4</b>	-0,11	0,05	0,08	0,06
<b>5</b>	0,11	0,16	0,08	0,06
<b>6</b>	<b>0,32</b>	0,15	0,08	0,06
<b>7</b>	0,00	0,11	0,08	0,06
<b>8</b>	0,18	0,19	0,23	0,16
<b>9</b>	0,24	-0,23	0,15	0,11
<b>10</b>	0,18	-0,38	0,19	0,13
<b>11</b>	-0,22	-0,13	0,14	0,10
<b>14</b>	-0,30	-0,04	0,14	0,10
<b>15</b>	-0,31	-0,14	0,18	0,13
<b>OLKI</b>	0,01	0,08	0,07	0,05

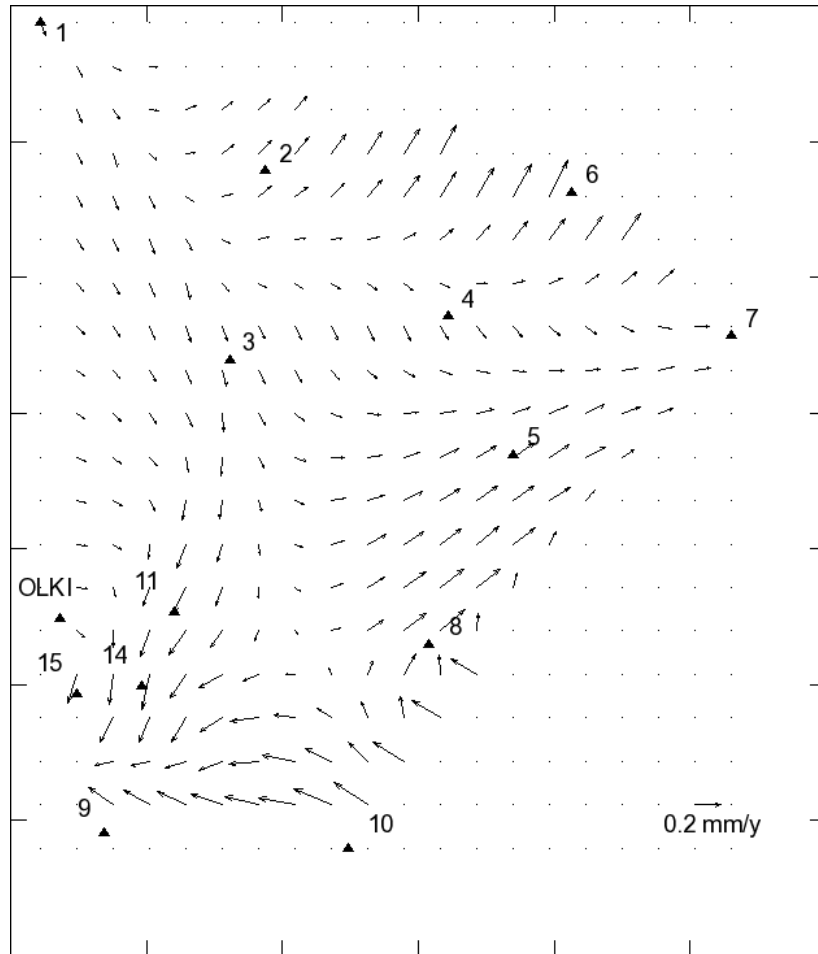


**Figure 6-7.** *The resulting velocity vector map of the deformation analysis. Especially the velocities of the southern part of the network are still uncertain due to short time series.*

In the second approach the deformation analysis was performed using only the northern pillars (1–7) and the Olkiluoto station, which have longer and therefore more reliable time series. The results of the first campaign (2003-1) were omitted from the analysis because of the outlying behaviour detected in many vectors. The results are presented in Table 6-2 and in Figure 6-8.

Now we could estimate statistically significant velocities for pillars 3 (Peräkulma), 6 (Sääksjärvi) and 7 (Järventausta). The estimated velocities are small (max 0.2 mm/a) but of the same order of magnitude than in Olkiluoto deformation studies (e.g. Ahola et al. 2008). The mean errors are slightly smaller than in the first analysis for the whole dataset. In addition the solution is not as sensitive to the GPS-processing strategy as in the first estimate. When overlaying the vectors with the geological information the possible change seems to take place in the vicinity of geologically interesting features, like the major shear zones (Figure 6-9).

The results are in line with simulation carried out by Kallio et al. (2009b), where it was estimated how well possible deformations can be detected from the data. According to

the analysis in five years data we will get on the level of 0.05 ppm, i.e. on a 30 km vector a 1.5 mm movement can be detected on a 99 % confidence level. To obtain more reliable results it is necessary to continue the research. More measurements campaigns are needed, especially to determine the deformation of the southern part of the network, but it is not necessary to carry out measurements as frequently.

**Table 6-2.** Results of the deformation analysis for the older part of the network (statistically significant velocities in bold).

	Velocity (mm/a)		Mean error (mm/a)	
	North	East	North	East
<b>1</b>	-0,08	-0,07	0,07	0,05
<b>2</b>	0,03	-0,06	0,07	0,04
<b>3</b>	-0,17	<b>-0,13</b>	0,06	0,04
<b>4</b>	-0,13	-0,02	0,06	0,04
<b>5</b>	0,04	0,07	0,07	0,04
<b>6</b>	<b>0,24</b>	0,04	0,07	0,05
<b>7</b>	0,00	<b>0,17</b>	0,08	0,05
<b>OLKI</b>	0,06	0,01	0,08	0,05

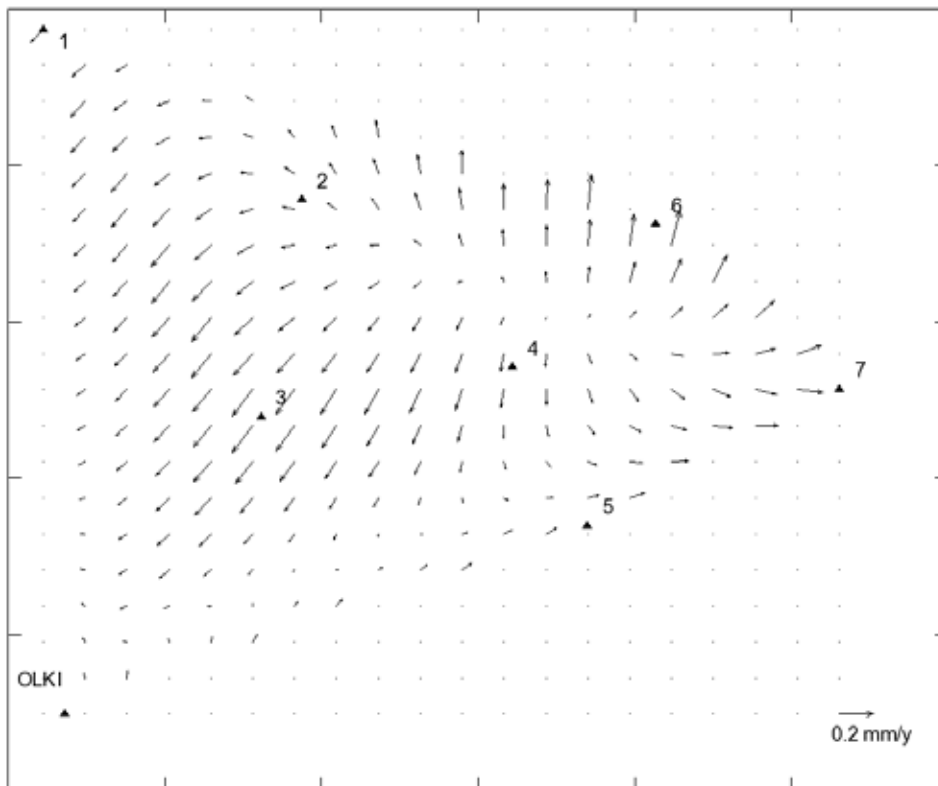


**Figure 6-8.** The velocity vector map for the Northern part of the network. The velocities of the pillars 3, 6 and 7 can be considered as statistically significant.

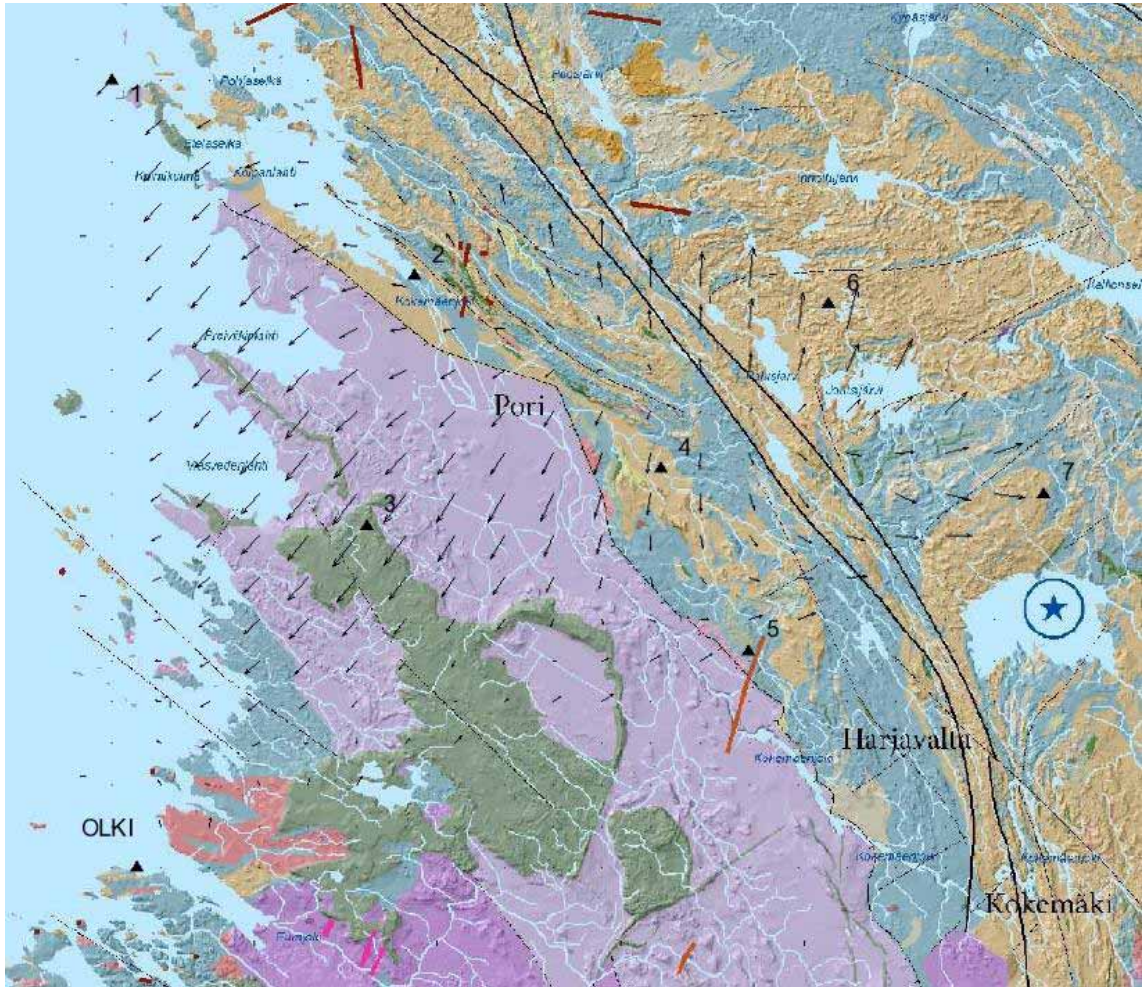


**Figure 6-9.** The estimated velocity vectors are slightly diverging in the vicinity of geologically interesting features, like the major shear zones (black solid lines) and Jotnian sandstone (see legend of Figure 1-1). Base map © Geological Survey of Finland.



## 7 CONCLUSIONS AND THE FUTURE

We have made three annual GPS campaigns in 2003–2008 to get a good and reliable start for the time series. It was decided that from 2009 onwards measurements will be done every 2-3 years. The current network covers the area of interest to obtain the movements in the area. We do not plan to add any new sites in the network. First, the number of points would increase too much to be manageable with current resources. Secondly, it would take many years before new points will give statistically equally significant results than the old ones, and therefore may disturb the analysis to be done in the network.

In five years we have reached the accuracy where any large movements can be excluded. There is, however, a possibility for 0.2-0.5 mm/y inter-station movements which can remain unobserved in the current data. Especially in the Southern part of the network, which is younger than the Northern part the time series are too short to draw any definite conclusions.

Another question is the mechanism of the possible movements. If the movements are abrupt events, happening only every now and then (and not necessarily accompanied by a detectable earthquake), one can see no movements at all during the quiet periods, but only a long-term monitoring will reveal them. This is a motivation to maintain the time series and continue observing campaigns regularly every few years.

The network is not only for geodynamics studies, but local authorities can use it for practical purposes as well. The network is the best possible reference for cities and municipalities in the area to tie their networks to the national reference frame, and this possibility has already been used quite extensively. Free access to the pillars were planned to serve specifically this purpose. Also for this purpose, long term stability and existence of the network is crucial.

We plan to continue our activities in the area also in the future. Observing campaigns in the network, combined with the activity at the Olkiluoto will be the basis of the research. We will also use existing gravity data and GPS-levelling results to compute a local geoid model, to fit it better in the sharp geoid features at the River Kokemäki. The Satakunta network is the first high-precision network in Finland of this size and therefore a valuable test field for geodetic techniques to detect minor deformations and network stability.



**ACKNOWLEDGEMENTS**

*The Cities of Pori and Rauma* are acknowledged for building the GPS observation pillars and helping us during the measurement campaigns. The project was partly funded by Satakuntaliitto and Academy of Finland, project RCD-Lito, 122822.



## REFERENCES

- Ahola, J., H. Koivula and J. Jokela (2008) GPS Operations at Olkiluoto, Kivetty and Romuvaara in 2007. Posiva Working Report 2008-35. 189 pages.
- Ahola, J., H. Koivula, M. Poutanen and J. Jokela (2007): GPS operations at Olkiluoto, Kivetty and Romuvaara in 2006. Working Report 2007-56. POSIVA Oy, Olkiluoto. 178 pages.
- Ahola, J. and M. Poutanen (2006): GPS-mittaukset Satakunnassa. GeoSatakunta 2005, Geologian tutkimuskeskus, Raportti P 34.4.043, Ed. Huhta, P., Espoo. Pages 8-16. (In Finnish)
- Bilker-Koivula, M., Ollikainen, M. (2009): Suomen geoidimallit ja niiden käyttäminen korkeuden muunnoksissa, Tiedote 29, Geodeettinen laitos (in Finnish)
- Cai, J., H. Koivula, E.W. Grafarend, M. Poutanen (2007): The statistical analysis of the eigenspace components of the strain rate tensor derived from FinnRef GPS measurements (1997-2004) in Fennoscandia. In: Xu P, J Liu and A Dermanis (Eds.): Proc. IAG Symposia 132. VI Hotine-Marussi Symposium of Theoretical and Computational Geodesy: Challenge and Role of Modern Geodesy, Wuhan, China, 29.5.-2.6.2006, pp. 79-87, Springer, Berlin, Heidelberg.
- Chen, R. (1991): On the horizontal crustal deformations in Finland. Reports of the Finnish Geodetic Institute 91:1. 98 pages.
- Chen, R. and Kakkuri, J. (1995). GPS work at Olkiluoto for the year 1994. Work Report PATU-95-30e, Posiva Oy, Helsinki. 11 pages.
- Dach, R., U. Hugentobler, P. Fridez and M. Meindl (2007): Bernese GPS software v. 5.0. University of Berne.
- DynaQlim (2008): Upper Mantle Dynamics and Quaternary Climate in Cratonic Areas. International Lithosphere Program (ILP) Regional Co-ordination Committee CC 1/5. <http://dynaqlim.fgi.fi/> (2008-05-07)
- Hutri, K-L. (2007): An approach to palaeoseismicity in the Olkiluoto (sea) area during the early Holocene. PhD. Thesis. STUK-A222 / JUNE 2007.
- IGS (2008): International GNSS Service. <http://igsceb.jpl.nasa.gov/> (2008-05-07)
- Johansson, J.M., Davis, J.L., Scherneck, H-G., Milne, G.A., Vermeer, M., Mitrovica, J.X., Bennett, R. A., Jonsson, B., Elgered, G., Elösegui, P., Koivula, H., Poutanen, M., Rønnang, B.O. and Shapiro, I.I. (2002): Continuous GPS measurements of postglacial adjustment in Fennoscandia 1. Geodetic results, *J. Geophys. Res.*, 107, DOI 10.1029/2001JB000400.
- Kakkuri J. (Ed.) (1994): Final Results of the Baltic Sea Level 1990 GPS Campaign, Rep. Finn. Geod. Inst. 94:2
- Kakkuri J. (Ed.) (1995): Final Results of the Baltic Sea Level 1993 GPS Campaign, Rep. Finn. Geod. Inst. 95:2
- Kakkuri, J. and M. Poutanen (1997): Geodetic Determination of the Surface Topography of the Baltic Sea. *Marine Geodesy* 20, no 4, 307-316

- Kallio, U., J. Ahola, H. Koivula, J. Jokela and M. Poutanen (2009a): GPS Operations at Olkiluoto, Kivetty and Romuvaara in 2008. Working Report 2009-75. POSIVA Oy, Olkiluoto.
- Kallio, U., M. Poutanen, H. Koivula, P. Lehmuskoski, J. Jokela, H. Ruotsalainen, M. Bilker-Koivula and P. Häkli (2009b): Olkiluodon geodeettisten mittausten kehittämissuunnitelma. A report to Posiva, May 5, 2009.
- Koivula, H. (2006): Implementation and Prospects for Use of a High Precision Geodetic GPS Monitoring Network (FinnRef) Covering Finland. Licentiate's Thesis. Helsinki University of Technology.
- Lambeck, K. and A. Purcell (2003): Glacial Rebound and Crustal Stress in Finland. Report 2003-10. Posiva Oy.
- Lehmuskoski, P. (2004): Precise Levelling of the Olkiluoto GPS Network in 2003. Working Report 2004-07. POSIVA Oy, Olkiluoto. 125 pages.
- Lehmuskoski, P. (2006): Precise Levelling of the Olkiluoto GPS Network in 2005. Working Report 2006-27. POSIVA Oy, Olkiluoto. 143 pages.
- Lehmuskoski, P. (2008): Precise Levelling of the Olkiluoto GPS Network in 2007. Working Report 2008-19. POSIVA Oy, Olkiluoto.
- Lidberg, M. (2007): Geodetic Reference Frames in Presence of Crustal Deformations. Doctoral Thesis. Department of Radio and Space Science, Chalmers University of Technology, Gothenburg, Sweden.
- Lidberg, M., J. M. Johansson and H-G. Scherneck (2006): Geodetic reference frames in the presence of crustal deformations - with focus on Nordic conditions. Symposium of the IAG subcommission for Europe (EUREF), June 14-17, Riga, 2006.
- Mäkinen, J., H. Koivula, M. Poutanen and V. Saaranen, (2003): Vertical Velocities in Finland from Permanent GPS Networks and from Repeated Precise Levelling. *Journal of Geodynamics*, Vol 35, No.4-5, pp. 443-456.
- Milne, G.A., J.L. Davis, J.X. Mitrovica, H.-G. Scherneck, J.M. Johansson, M. Vermeer and H. Koivula (2001): Space-Geodetic Constraints on Glacial Isostatic Adjustment in Fennoscandia. *Science*, Vol. 291, p. 2381-2385.
- Milne, G.A., J.X. Mitrovica, H.-G. Scherneck, J.L. Davis, J.M. Johansson, H. Koivula and M. Vermeer (2004). Continuous GPS measurements of postglacial adjustment in Fennoscandia: 2. Modelling results. *Journal of Geophysical Research*. 109, No. B2.
- Ollikainen, M. and J. Kakkuri (1999): GPS operations at Olkiluoto, Kivetty and Romuvaara for 1998. Working Report 99-31. Posiva Oy, Helsinki, 134 pages.
- Ollikainen, M., H. Koivula, M. Poutanen and R. Chen (1997): Suomen kiinteiden GPS-asemien verkko. Geodeettisen laitoksen tiedote no. 16. 34 s. (In Finnish)
- Paulamäki, S., M. Paananen and S. Elo (2002): Structure and geological evolution of the bedrock of southern Satakunta, SW Finland. Report 2002-04. Posiva Oy.
- Poutanen, M. (2000): Sea surface topography and vertical datums using space geodetic techniques. *Publications of the Finnish Geodetic Institute*, 128, 158 pp.

Poutanen, M. (2005): Geodetic measurements. Bedrock stress field in the Satakunta region. Geological Survey of Finland, Report P 34.4.042. Editors P. Huhta, and K. Korsman.

Poutanen, M. and J. Kakkuri (Ed.) (1999): Final results of the Baltic Sea Level 1997 GPS campaign. Rep. Finn. Geod. Inst. 99:4, 182 p.

Poutanen, M., P. Knudsen, M. Lilje, T. Nørbech, H.- P. Plag and H.-G. Scherneck (2005): NGOS – The Nordic Geodetic Observing System. Nordic Journal of Surveying and Real Estate Research. Vol 2, No 2, pp. 79-100.

Poutanen, M. and the National Lithosphere Committee (2006): Upper mantle dynamics and Quaternary climate in cratonic areas: A proposal for an ILP project. Fourth Symposium on the structure, composition and evolution of the Lithosphere in Finland (Ed. I.T. Kukkonen, O. Eklund, A. Korja, T. Korja, L.J. Pesonen, M. Poutanen). Geological Survey of Finland, Espoo. 155-156.

Poutanen M., D. Dransch, S. Gregersen, S. Haubrock, E.R. Ivins, V. Klemann, E. Kozlovskaya, I. Kukkonen, B. Lund, J.-P. Lunkka, G. Milne, J. Müller, C. Pascal, B.R. Pettersen, H.-G. Scherneck, H. Steffen, B. Vermeersen, D. Wolf (2009): DynaQlim – Upper Mantle Dynamics and Quaternary Climate in Cratonic Areas. Accepted for ILP volume "New Frontiers in Integrated Solid Earth Sciences" (Cloetingh, S and Nengendank, J. (Eds.). Springer Verlag.

Poutanen, M., P. Knudsen, M. Lilje, T. Nørbech, H.- P. Plag and H.-G. Scherneck, (2007): The Nordic Geodetic Observing System (NGOS). In Dynamic Planet - Monitoring and Understanding a Dynamic Planet with Geodetic and Oceanographic Tools, Conference of the International Association of Geodesy 22-26 August 2005, Cairns, Australia (Ed. C. Rizos and P. Tregoning), International Association of Geodesy Symposia , Vol. 130: 749-756.

Poutanen M. and J. Ahola (2010): Maankuoren liiketutkimukset Satakunnassa GPS-mittausten avulla. (in Finnish) – coming to GSF publication series.

Seismo (2007): Map of earthquake locations in Finland 1965-  
<http://www.seismo.helsinki.fi/fi/bulletiinit/mjt1965-nyt.html>

Scherneck, H.-G., J.M. Johansson, G. Elgered, J.L. Davis, B. Jonsson, G. Hedling, H. Koivula, M. Ollikainen, M. Poutanen, M. Vermeer, J.X. Mitrovica, and G.A. Milne (2002): BIFROST: Observing the Three-Dimensional Deformation of Fennoscandia. In Ice Sheets, Sea Level and the Dynamic Earth, (Eds. J.X. Mitrovica and B.L.A. Vermeersen). American Geophysical Union, Geodynamics Series, Volume 29, Washington, D.C., p. 69-93.

Vestøl, O. (2006): Determination of postglacial land uplift in Fennoscandia from leveling, tide-gauges and continuous GPS stations using least squares collocation. Journal of Geodesy 80, 248-258. doi 10.1007/s00190-006-0063-7.

Ågren, J. and R. Svensson (2007): Postglacial Land Uplift Model and System Definition for the New Swedish Height System RH 2000. Lantmäteriet, Rapportserie: Geodesi och Geografiska informationssystem, 2007:4, Gävle. 124 p.



**APPENDIX 1**

*Computed vectors (m)*

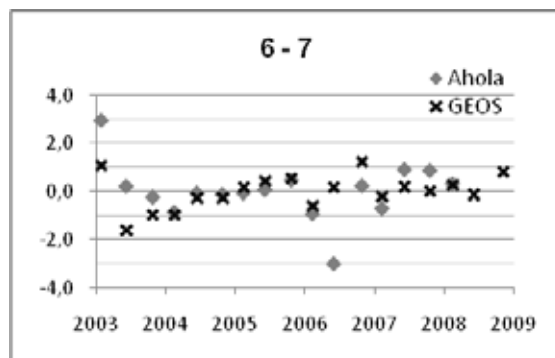
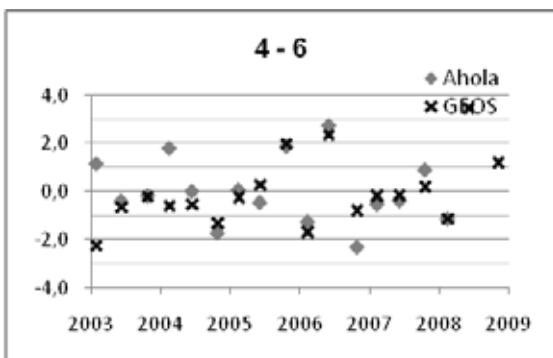
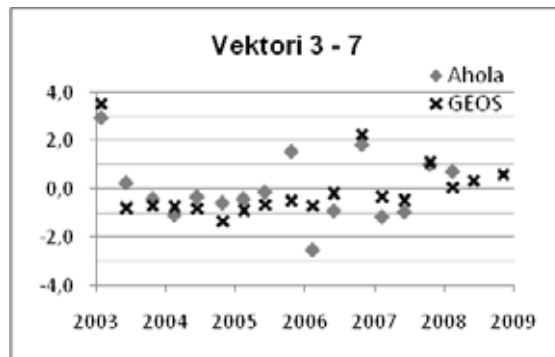
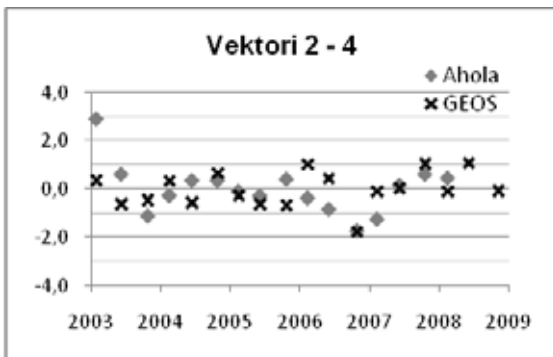
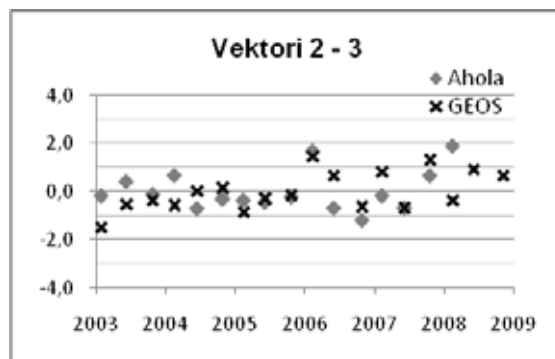
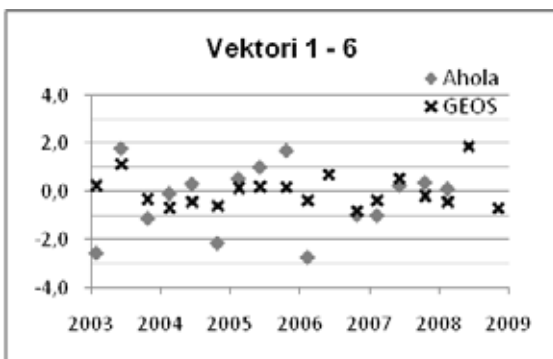
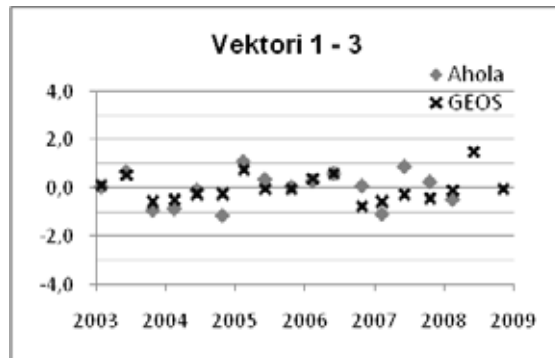
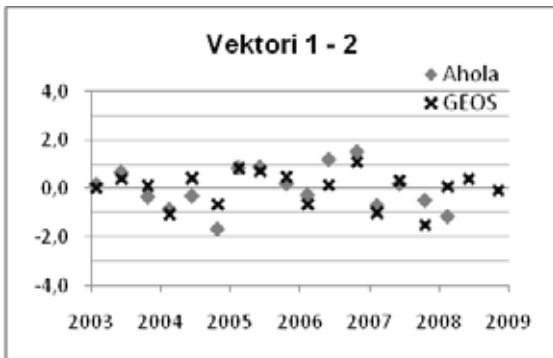
		2003-1	2003-2	2003-3	2004-1	2004-2	2004-3	2005-1	2005-2	2005-3	2006-1	2006-2	2006-3	2007-1	2007-2	2007-3	2008-1	2008-2	2008-3
Date		21.-25.1.	2.-3.6.	20.-21.10.	10.-11.2.	8.-9.6.	20.-21.10.	8.-9.2.	1.-2.6.	17.-20.10.	6.-9.2.	29.5.-1.6.	23.-26.10.	5.-8.2.	4.-7.6.	15.-18.10.	11.-14.2.	2.-5.6.	3.-6.11.
DOY		021-025	153-154	293-294	041-042	160-161	294-295	039-040	152-153	290-293	037-040	149-152	296-299	036-039	155-158	288-291	042-045	154-157	308-311
Time		2003.0630	2003.4210	2003.8040	2004.1140	2004.4400	2004.8070	2005.1080	2005.4180	2005.8000	2006.1040	2006.4110	2006.8164	2007.1041	2007.4274	2007.7945	2008.1205	2008.4274	2008.8493
1	1-2	19763.7521	19763.7525	19763.7522	19763.7510	19763.7525	19763.7514	19763.7529	19763.7528	19763.7525	19763.7514	19763.7522	19763.7531	19763.7511	19763.7524	19763.7506	19763.7521	19763.7525	19763.7520
2	1-3	28408.6086	28408.6090	28408.6079	28408.6079	28408.6082	28408.6082	28408.6092	28408.6084	28408.6084	28408.6088	28408.6090	28408.6077	28408.6079	28408.6082	28408.6080	28408.6083	28408.6100	28408.6084
3	1-4	36885.8927	36885.8920	36885.8918	36885.8915	36885.8920	36885.8922	36885.8928	36885.8923	36885.8920	36885.8925	36885.8927	36885.8915	36885.8910	36885.8925	36885.8917	36885.8922	36885.8936	36885.8920
4	1-5	47058.5537	47058.5524	47058.5534	47058.5528	47058.5506	47058.5543	47058.5536	47058.5519	47058.5519	47058.5533	47058.5527	47058.5525	47058.5533	47058.5540	47058.5519	47058.5529	47058.5534	47058.5524
5	1-6	40976.1771	40976.1780	40976.1765	40976.1762	40976.1764	40976.1763	40976.1770	40976.1770	40976.1770	40976.1765	40976.1775	40976.1760	40976.1765	40976.1774	40976.1767	40976.1764	40976.1787	40976.1762
6	1-7	55753.9436	55753.9410	55753.9400	55753.9397	55753.9403	55753.9402	55753.9413	55753.9410	55753.9407	55753.9405	55753.9412	55753.9421	55753.9403	55753.9415	55753.9409	55753.9410	55753.9419	55753.9410
7	1-8												53857.9812	53857.9805	53857.9821	53857.9817	53857.9811	53857.9815	53857.9814
8	1-9								59730.1630	59730.1629	59730.1626	59730.1632	59730.1608	59730.1606	59730.1622	59730.1627	59730.1621	59730.1611	59730.1619
9	1-10										64755.6740	64755.6719	64755.6717	64755.6716	64755.6722	64755.6735	64755.6721	64755.6716	64755.6716
10	1-11								44418.3786	44418.3794	44418.3800	44418.3782	44418.3788	44418.3791	44418.3790	44418.3791	44418.3796	44418.3793	44418.3793
11	1-14								49372.2194	49372.2198	49372.2204	49372.2200	49372.2193	49372.2209	49372.2189	49372.2195	49372.2204	49372.2204	49372.2204
12	1-15								49423.0455	49423.0464	49423.0462	49423.0461	49423.0461	49423.0462	49423.0458	49423.0466	49423.0467	49423.0459	49423.0459
13	1-OLKI	43820.4452	43820.4457	43820.4452	43820.4455	43820.4445	43820.4455	43820.4463	43820.4458	43820.4445	43820.4465	43820.4463	43820.4448	43820.4453	43820.4444	43820.4437	43820.4452	43820.4459	43820.4446
14	2-3	14111.5549	14111.5559	14111.5560	14111.5558	14111.5564	14111.5565	14111.5556	14111.5561	14111.5563	14111.5578	14111.5570	14111.5558	14111.5572	14111.5557	14111.5577	14111.5560	14111.5573	14111.5570
15	2-4	17158.7976	17158.7967	17158.7969	17158.7976	17158.7967	17158.7980	17158.7970	17158.7967	17158.7966	17158.7983	17158.7977	17158.7956	17158.7972	17158.7973	17158.7983	17158.7972	17158.7984	17158.7972
16	2-5	27709.0374	27709.0361	27709.0376	27709.0381	27709.0345	27709.0395	27709.0367	27709.0354	27709.0357	27709.0385	27709.0366	27709.0357	27709.0387	27709.0380	27709.0377	27709.0369	27709.0370	27709.0368
17	2-6	22605.1981	22605.1980	22605.1967	22605.1977	22605.1962	22605.1970	22605.1970	22605.1970	22605.1975	22605.1967	22605.1981	22605.1955	22605.1975	22605.1975	22605.1982	22605.1969	22605.1994	22605.1967
18	2-7	36373.0635	36373.0599	36373.0591	36373.0602	36373.0590	36373.0599	36373.0598	36373.0594	36373.0594	36373.0601	36373.0602	36373.0603	36373.0603	36373.0615	36373.0602	36373.0608	36373.0602	36373.0602
19	2-8												36810.3389	36810.3397	36810.3405	36810.3422	36810.3392	36810.3391	36810.3400
20	2-9								50054.3870	50054.3877	50054.3871	50054.3870	50054.3858	50054.3847	50054.3878	50054.3863	50054.3850	50054.3864	50054.3864
21	2-10										50167.4955	50167.4928	50167.4943	50167.4929	50167.4953	50167.4948	50167.4935	50167.4935	50167.4935
22	2-11								33088.8523	33088.8542	33088.8538	33088.8516	33088.8539	33088.8527	33088.8544	33088.8527	33088.8533	33088.8534	33088.8534
23	2-14								38980.2855	38980.2864	38980.2867	38980.2858	38980.2861	38980.2869	38980.2862	38980.2851	38980.2862	38980.2862	38980.2867
24	2-15								40850.6399	40850.6415	40850.6408	40850.6402	40850.6417	40850.6405	40850.6415	40850.6407	40850.6408	40850.6407	40850.6407
25	2-OLKI	36202.8756	36202.8781	36202.8786	36202.8777	36202.8781	36202.8786	36202.8779	36202.8790	36202.8775	36202.8800	36202.8794	36202.8775	36202.8790	36202.8777	36202.8779	36202.8777	36202.8784	36202.8778
26	3-4	16304.9903	16304.9882	16304.9886	16304.9886	16304.9889	16304.9890	16304.9885	16304.9892	16304.9888	16304.9893	16304.9885	16304.9894	16304.9887	16304.9888	16304.9896	16304.9895	16304.9889	16304.9887
27	3-5	21961.2222	21961.2203	21961.2220	21961.2209	21961.2198	21961.2216	21961.2212	21961.2207	21961.2204	21961.2209	21961.2216	21961.2220	21961.2221	21961.2218	21961.2210	21961.2215	21961.2213	21961.2212
28	3-6	27990.8824	27990.8822	27990.8823	27990.8820	27990.8822	27990.8817	27990.8820	27990.8834	27990.8844	27990.8817	27990.8842	27990.8826	27990.8829	27990.8825	27990.8838	27990.8824	27990.8857	27990.8834
29	3-7	36921.4325	36921.4282	36921.4283	36921.4283	36921.4282	36921.4277	36921.4281	36921.4284	36921.4285	36921.4283	36921.4288	36921.4312	36921.4287	36921.4285	36921.4301	36921.4290	36921.4293	36921.4296
30	3-8												25514.6014	25514.6006	25514.6017	25514.6014	25514.6006	25514.5994	25514.6009

	2003-1	2003-2	2003-3	2004-1	2004-2	2004-3	2005-1	2005-2	2005-3	2006-1	2006-2	2006-3	2007-1	2007-2	2007-3	2008-1	2008-2	2008-3	
Date	21.-25.1.	2.-3.6.	20.-21.10.	10.-11.2.	8.-9.6.	20.-21.10.	8.-9.2.	1.-2.6.	17.-20.10.	6.-9.2.	29.5.-1.6.	23.-26.10.	5.-8.2.	4.-7.6.	15.-18.10.	11.-14.2.	2.-5.6.	3.-6.11.	
DOY	021-025	153-154	293-294	041-042	160-161	294-295	039-040	152-153	290-293	037-040	149-152	296-299	036-039	155-158	288-291	042-045	154-157	308-311	
Time	2003.0630	2003.4210	2003.8040	2004.1140	2004.4400	2004.8070	2005.1080	2005.4180	2005.8000	2006.1040	2006.4110	2006.8164	2007.1041	2007.4274	2007.7945	2008.1205	2008.4274	2008.8493	
31	3-9								35971.5274	35971.5266	35971.5268	35971.5278	35971.5253	35971.5257	35971.5268	35971.5270	35971.5245	35971.5261	
32	3-10											36953.5663	36953.5654	36953.5648	36953.5654	36953.5665	36953.5636	36953.5645	
33	3-11							18981.5413	18981.5417	18981.5420	18981.5410	18981.5419	18981.5422	18981.5419	18981.5419	18981.5419	18981.5412	18981.5416	
34	3-14							24897.3370	24897.3364	24897.3375	24897.3377	24897.3367	24897.3390	24897.3362	24897.3368	24897.3368	24897.3367	24897.3374	
35	3-15							27015.0775	27015.0776	27015.0777	27015.0778	27015.0783	27015.0786	27015.0777	27015.0785	27015.0775	27015.0775	27015.0774	
36	3-OLKI	22780.0881	22780.0899	22780.0900	22780.0894	22780.0891	22780.0897	22780.0898	22780.0902	22780.0887	22780.0897	22780.0900	22780.0886	22780.0892	22780.0896	22780.0879	22780.0891	22780.0889	22780.0881
37	4-5	11246.1798	11246.1785	11246.1798	11246.1801	11246.1767	11246.1814	11246.1787	11246.1779	11246.1782	11246.1798	11246.1771	11246.1792	11246.1806	11246.1800	11246.1787	11246.1792	11246.1772	11246.1783
38	4-6	12932.6596	12932.6612	12932.6616	12932.6612	12932.6613	12932.6605	12932.6615	12932.6621	12932.6638	12932.6601	12932.6641	12932.6610	12932.6616	12932.6616	12932.6620	12932.6607	12932.6652	12932.6630
39	4-7	20933.0818	20933.0798	20933.0792	20933.0792	20933.0790	20933.0784	20933.0793	20933.0789	20933.0794	20933.0787	20933.0798	20933.0815	20933.0797	20933.0794	20933.0802	20933.0793	20933.0799	20933.0804
40	4-8												24125.7079	24125.7063	24125.7084	24125.7094	24125.7076	24125.7051	24125.7066
41	4-9							45551.0859	45551.0854	45551.0849	45551.0864	45551.0840	45551.0841	45551.0862	45551.0859	45551.0834	45551.0843	45551.0843	
42	4-10										39777.9913	39777.9911	39777.9909	39777.9900	39777.9915	39777.9927	39777.9898	39777.9898	
43	4-11							29558.5426	29558.5435	29558.5425	29558.5423	29558.5433	29558.5428	29558.5439	29558.5439	29558.5430	29558.5430	29558.5423	
44	4-14							35292.3803	35292.3798	35292.3801	35292.3809	35292.3796	35292.3816	35292.3800	35292.3805	35292.3805	35292.3802	35292.3799	
45	4-15							38862.1902	38862.1906	38862.1899	38862.1906	38862.1911	38862.1908	38862.1912	38862.1912	38862.1917	38862.1904	38862.1898	
46	4-OLKI	36140.9004	36140.9009	36140.9008	36140.8999	36140.9004	36140.9008	36140.9004	36140.9018	36140.9001	36140.9010	36140.9006	36140.9001	36140.9002	36140.9007	36140.9001	36140.9008	36140.9002	36140.8990
47	5-6	19783.5638	19783.5628	19783.5649	19783.5658	19783.5625	19783.5670	19783.5642	19783.5643	19783.5663	19783.5649	19783.5641	19783.5641	19783.5654	19783.5656	19783.5650	19783.5644	19783.5657	19783.5653
48	5-7	18288.0235	18288.0201	18288.0200	18288.0216	18288.0194	18288.0211	18288.0193	18288.0190	18288.0202	18288.0210	18288.0184	18288.0218	18288.0199	18288.0202	18288.0216	18288.0203	18288.0196	18288.0208
49	5-8											15248.7394	15248.7362	15248.7390	15248.7409	15248.7387	15248.7390	15248.7387	
50	5-9							40912.2255	40912.2233	40912.2278	40912.2261	40912.2234	40912.2235	40912.2256	40912.2256	40912.2250	40912.2260	40912.2250	
51	5-10										31389.7144	31389.7113	31389.7098	31389.7092	31389.7114	31389.7122	31389.7128	31389.7109	
52	5-11							27435.1396	27435.1391	27435.1420	27435.1398	27435.1403	27435.1396	27435.1404	27435.1405	27435.1405	27435.1424	27435.1401	
53	5-14							32190.3362	32190.3339	32190.3387	32190.3368	32190.3351	32190.3367	32190.3354	32190.3358	32190.3384	32190.3363		
54	5-15							36546.8283	36546.8271	36546.8309	36546.8289	36546.8291	36546.8285	36546.8288	36546.8292	36546.8307	36546.8288		
55	5-OLKI	35454.2919	35454.2935	35454.2937	35454.2909	35454.2930	35454.2912	35454.2933	35454.2940	35454.2923	35454.2916	35454.2953	35454.2927	35454.2926	35454.2931	35454.2922	35454.2927	35454.2944	35454.2922
56	6-7	15793.6776	15793.6749	15793.6756	15793.6756	15793.6763	15793.6763	15793.6767	15793.6770	15793.6771	15793.6760	15793.6767	15793.6763	15793.6767	15793.6765	15793.6768	15793.6764	15793.6773	
57	6-8											34861.2147	34861.2129	34861.2158	34861.2173	34861.2143	34861.2160	34861.2154	
58	6-9							58285.5184	58285.5142	58285.5179	58285.5161	58285.5142	58285.5145	58285.5169	58285.5153	58285.5176	58285.5176		
59	6-10										50981.0217	50981.0184	50981.0183	50981.0180	50981.0197	50981.0198	50981.0216	50981.0193	
60	6-11							42484.3379	42484.3351	42484.3381	42484.3348	42484.3363	42484.3359	42484.3373	42484.3360	42484.3397	42484.3368		

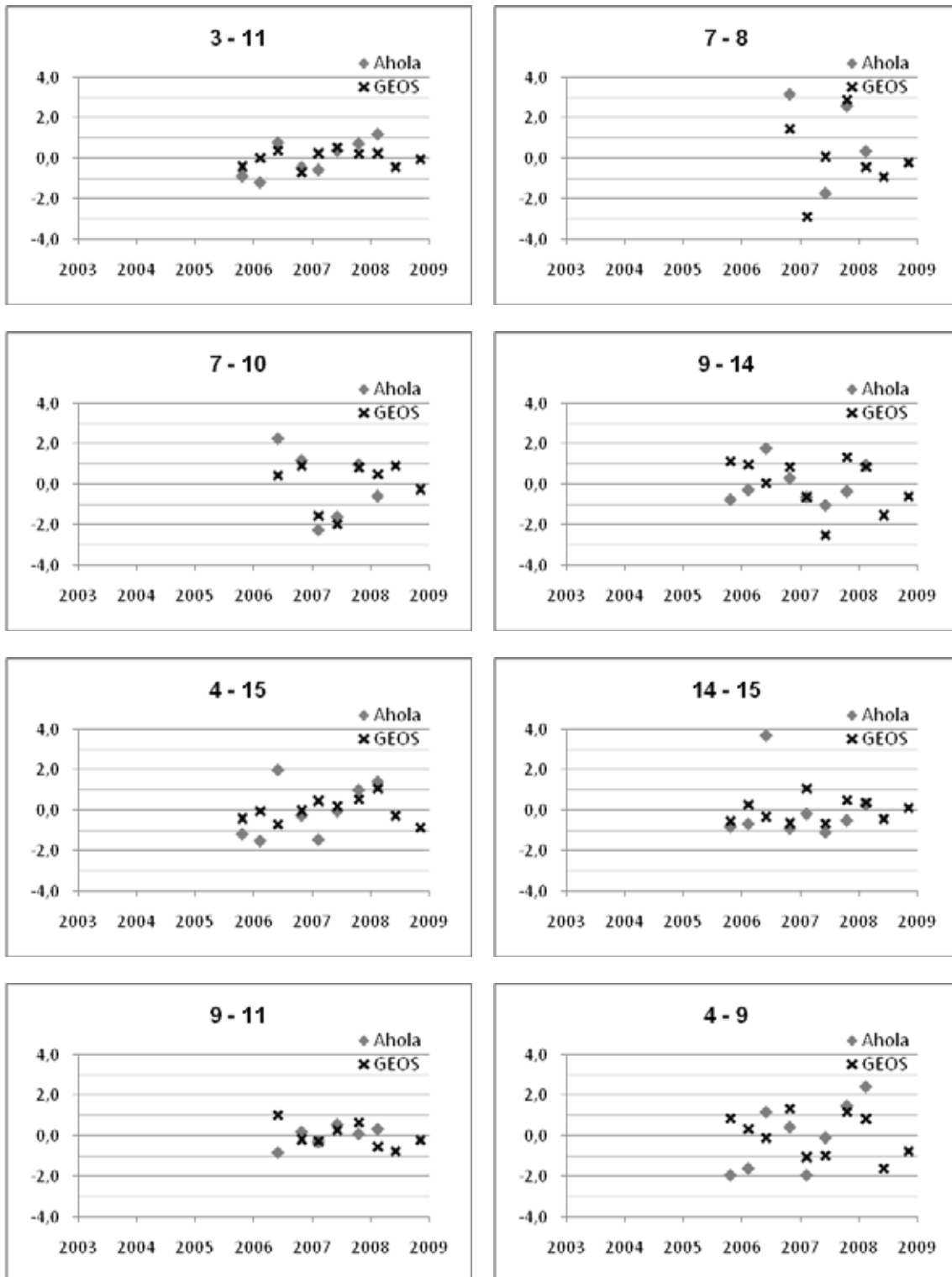
	2003-1	2003-2	2003-3	2004-1	2004-2	2004-3	2005-1	2005-2	2005-3	2006-1	2006-2	2006-3	2007-1	2007-2	2007-3	2008-1	2008-2	2008-3	
Date	21.-25.1.	2.-3.6.	20.-21.10.	10.-11.2.	8.-9.6.	20.-21.10.	8.-9.2.	1.-2.6.	17.-20.10.	6.-9.2.	29.5.-1.6.	23.-26.10.	5.-8.2.	4.-7.6.	15.-18.10.	11.-14.2.	2.-5.6.	3.-6.11.	
DOY	021-025	153-154	293-294	041-042	160-161	294-295	039-040	152-153	290-293	037-040	149-152	296-299	036-039	155-158	288-291	042-045	154-157	308-311	
Time	2003,0630	2003,4210	2003,8040	2004,1140	2004,4400	2004,8070	2005,1080	2005,4180	2005,8000	2006,1040	2006,4110	2006,8164	2007,1041	2007,4274	2007,7945	2008,1205	2008,4274	2008,8493	
61	6-14								48182,8675	48182,8632	48182,8676	48182,8652	48182,8645	48182,8665	48182,8653	48182,8645	48182,8688	48182,8662	
62	6-15								51794,4251	51794,4218	51794,4251	51794,4227	51794,4238	51794,4236	51794,4242	51794,4235	51794,4267	51794,4239	
63	6-OLKI	48999,6506	48999,6527	48999,6529	48999,6517	48999,6522	48999,6518	48999,6525	48999,6544	48999,6543	48999,6517	48999,6551	48999,6516	48999,6525	48999,6528	48999,6526	48999,6520	48999,6558	48999,6524
64	7-8											31781,4967	31781,4924	31781,4953	31781,4981	31781,4948	31781,4943	31781,4950	
65	7-9								58813,0639	58813,0629	58813,0645	58813,0661	58813,0620	58813,0623	58813,0656	58813,0636	58813,0641	58813,0642	
66	7-10										47082,5516	47082,5521	47082,5497	47082,5492	47082,5520	47082,5517	47082,5521	47082,5510	
67	7-11								45700,5841	45700,5844	45700,5849	45700,5859	45700,5845	45700,5840	45700,5864	45700,5851	45700,5863	45700,5853	
68	7-14								50457,7772	50457,7759	50457,7780	50457,7795	50457,7761	50457,7779	50457,7780	50457,7770	50457,7790	50457,7780	
69	7-15								54834,7600	54834,7597	54834,7609	54834,7622	54834,7606	54834,7603	54834,7620	54834,7611	54834,7619	54834,7611	
70	7-OLKI	53602,2616	53602,2599	53602,2598	53602,2586	53602,2590	53602,2582	53602,2589	53602,2596	53602,2589	53602,2588	53602,2602	53602,2608	53602,2587	53602,2594	53602,2601	53602,2592	53602,2604	53602,2593
71	8-9											27559,7671	27559,7675	27559,7652	27559,7655	27559,7664	27559,7677	27559,7671	
72	8-10											16147,7617	16147,7633	16147,7600	16147,7602	16147,7633	16147,7636	16147,7619	
73	8-11											18826,6360	18826,6378	18826,6358	18826,6357	18826,6365	18826,6378	18826,6367	
74	8-14											21326,2363	21326,2370	21326,2362	21326,2344	21326,2358	21326,2380	21326,2366	
75	8-15											26086,6690	26086,6714	26086,6688	26086,6682	26086,6695	26086,6709	26086,6699	
76	8-OLKI											27206,4590	27206,4603	27206,4598	27206,4584	27206,4590	27206,4603	27206,4595	
77	9-10										17904,7440	17904,7428	17904,7427	17904,7433	17904,7436	17904,7424	17904,7422	17904,7428	
78	9-11								17027,3986	17027,3974	17027,3973	17027,3994	17027,3959	17027,3961	17027,3975	17027,3975	17027,3957	17027,3970	
79	9-14								11075,0393	11075,0391	11075,0382	11075,0390	11075,0375	11075,0356	11075,0395	11075,0390	11075,0366	11075,0376	
80	9-15								10391,0069	10391,0060	10391,0058	10391,0065	10391,0043	10391,0038	10391,0058	10391,0057	10391,0039	10391,0055	
81	9-OLKI								16092,4112	16092,4091	16092,4091	16092,4110	16092,4084	16092,4090	16092,4111	16092,4103	16092,4079	16092,4099	
82	10-11										21541,0640	21541,0636	21541,0633	21541,0625	21541,0636	21541,0645	21541,0626	21541,0625	
83	10-14										19249,6841	19249,6827	19249,6827	19249,6822	19249,6834	19249,6838	19249,6822	19249,6819	
84	10-15										22885,0981	22885,0964	22885,0972	22885,0965	22885,0974	22885,0975	22885,0959	22885,0966	
85	10-OLKI										27100,0339	27100,0328	27100,0326	27100,0336	27100,0340	27100,0337	27100,0317	27100,0326	
86	11-14								6005,9744	6005,9732	6005,9741	6005,9753	6005,9732	6005,9754	6005,9729	6005,9735	6005,9740	6005,9744	
87	11-15								9358,3644	9358,3639	9358,3643	9358,3650	9358,3646	9358,3648	9358,3641	9358,3646	9358,3642	9358,3643	
88	11-OLKI								8478,2699	8478,2692	8478,2705	8478,2698	8478,2692	8478,2708	8478,2694	8478,2692	8478,2692	8478,2695	
89	14-15								4762,6579	4762,6587	4762,6581	4762,6579	4762,6595	4762,6578	4762,6590	4762,6589	4762,6581	4762,6586	
90	14-OLKI								7852,3756	7852,3750	7852,3754	7852,3757	7852,3755	7852,3771	7852,3763	7852,3755	7852,3751	7852,3763	
91	15-OLKI								5704,0541	5704,0529	5704,0530	5704,0543	5704,0538	5704,0549	5704,0550	5704,0543	5704,0537	5704,0542	

## APPENDIX 2

Vector time series between neighbouring stations Y-axis is the deviation from the mean (mm).



Vector time series from the southern part of the network.



Vector time series from Olkiluoto station.

